Phylogenomics, trophic ecology, and systematics of the truffle-forming *Morchellaceae*

B. Lemmond^{1*}, G. Bonito², R. Healy¹, J. Van Wyk², H.A. Dawson³, C.R. Noffsinger⁴, R. Stephens⁵, A. Sow², J.M. Trappe⁶, T. Orihara⁷, P. Mleczko⁸, V. Kaounas⁹, M.E. Smith^{1*}

Key words:

ectomycorrhizal fungi fungal systematics hypogeous fungi mycophagy new taxa Pezizales stable isotopes Abstract: The family Morchellaceae contains four truffle-forming genera: Fischerula, Imaia, Kalapuya, and Leucangium. In North America, some Imaia, Kalapuya, and Leucangium species are highly regarded gourmet edible fungi. In this study, we address longstanding questions about the evolution, systematics, and trophic mode of these fungal genera. We used high-throughput sequencing and a custom genome assembly pipeline to sequence and assemble 41 new genomes of epigeous and hypogeous Morchellaceae genera and outgroup taxa from the sister family Discinaceae. Phylogenomic reconstructions based on high-quality de novo genomes and published reference genomes support a single transition from epigeous to hypogeous habit within the Morchellaceae. These results are corroborated by phylogenetic evidence from LSU, tef1, and rpb2 with a larger dataset of specimens and publicly available sequences. We also provide direct morphological and molecular evidence that one species of Leucangium from North America forms ectomycorrhizas on Pseudotsuga menziesii in a natural habitat. Stable isotope analysis further supports the hypothesis that other species of truffle-forming Morchellaceae also obtain carbon via ectomycorrhizal symbiosis. Phylogenetic and morphological analysis supports the description of two new species and one new combination of Leucangium as well as one new species and one new combination of Imaia from North America. We also discuss additional, undescribed diversity detected in our phylogenetic analyses of these genera derived from fungarium specimens, mycophagous mammal scat samples, and other environmental samples.

Citation: Lemmond B, Bonito G, Healy R, Van Wyk J, Dawson HA, Noffsinger CR, Stephens R, Sow A, Trappe JM, Orihara T, Mleczko P, Kaounas V, Smith ME (2025). Phylogenomics, trophic ecology, and systematics of the truffle-forming *Morchellaceae*. *Persoonia* **55**: 59–91. doi: 10.3114/persoonia.2025.55.02

Received: 28 May 2024; Accepted: 30 April 2025; Effectively published online: 31 July 2025

Corresponding editor: J. Houbraken

INTRODUCTION

The family Morchellaceae contains three genera of epigeous apothecial fungi (Disciotis, Morchella, and Verpa) and four genera of stereothecial, truffle-like fungi (Fischerula, Imaia, Kalapuya, and Leucangium). Although the family is perhaps best known around the world for the widely consumed and cultivated morels (Morchella spp.), over the past several decades certain Morchellaceae truffle genera have attracted increased attention both as culinary delicacies and through increased recognition of their global diversity. For example, a Leucangium species commonly referred to as L. carthusianum, or simply the "Oregon black truffle" (hereafter referred to as Leucangium cf. carthusianum), has been commercially harvested in the Pacific Northwest of North

America for decades and is perhaps the most commercially valuable native truffle species in North America (Trappe 2009, Lefevre 2012). Exact commercial volumes and sales figures are difficult to obtain, since harvest is generally conducted by individual collectors and sold directly to chefs and restaurants (Pilz & Molina 2002, B. Lemmond, pers. obs.). However, the popularity and availability of *Leucangium cf. carthusianum* and other truffles has spawned a unique network of regional events and industries. These include an annual local truffle festival (the Oregon Truffle Festival) which includes the "Joriad" truffle dog competition, several truffle dog training companies, numerous high-end food products made with local truffles, and restaurants that regularly feature local truffles on their menus (Czap 2012, Benitez 2021, Salvia 2023). On a far smaller scale, another hypogeous *Morchellaceae* species

© 2025 Westerdijk Fungal Biodiversity Institute

You are free to share - to copy, distribute and transmit the work, under the following conditions:

Attribution: You must attribute the work in the manner specified by the author or licensor (but not in any way that suggests that they endorse you or your use of the work). You may not use this work for commercial purposes.

No derivative works: You may not alter, transform, or build upon this work.

For any reuse or distribution, you must make clear to others the license terms of this work, which can be found at https://creativecommons.org/licenses/by-nc-nd/4.0/. Any of the above conditions can be waived if you get permission from the copyright holder. Nothing in this license impairs or restricts the author's moral rights.

¹Department of Plant Pathology, University of Florida, Gainesville, Florida 32611, USA

²Department of Plant, Soil and Microbial Sciences, Michigan State University, East Lansing, Michigan 48824, USA

³Institute of Ecology and Evolution, University of Oregon, Eugene, Oregon 97403, USA

⁴Department of Ecology and Evolutionary Biology, University of Tennessee, Knoxville, Tennessee 37996, USA

⁵Department of Biological Sciences, East Tennessee State University, Johnson City, Tennessee 37614, USA

⁶Department of Botany and Plant Pathology, Oregon State University, Corvallis, Oregon 97331, USA

⁷Kanagawa Prefectural Museum of Natural History, Odawara, Kanagawa 250-0031, Japan

⁸Institute of Botany, Faculty of Biology, Jagiellonian University in Kraków, Kraków 30-387, Poland

⁹Greek Mushroom Society, Sokratous 58, TK-19016 Artemis Attika, Greece

^{*}Corresponding authors: B. Lemmond, benlemmond@gmail.com; M.E. Smith, trufflesmith@ufl.edu

known as *Imaia gigantea* has recently gained a reputation as a culinary truffle that is harvested by a small number of collectors in the southern Appalachian Mountains in eastern North America (CNN 2022). *Imaia gigantea* is also traditionally harvested in some communities in parts of Japan (Yamada 2006). Outside of these cases, hypogeous *Morchellaceae* are infrequently recorded, although there are several other species described from Asia and Europe (discussed below in the Taxonomic Overview section). There are no reports of successful isolation or cultivation of any *Morchellaceae* truffle species.

Only a few morphological features indicate a link between hypogeous and epigeous Morchellaceae taxa, and some of the most taxonomically useful morphological features still require advanced microscopy techniques to observe them. An ultrastructural study of Leucangium cf. carthusianum from the Pacific Northwest by Li (1997) noted similarities between the cylindrical Woronin bodies and multinucleate ascospores of Leucangium and those in other epigeous Morchellaceae taxa. Other features, such as the septal pore type and spore morphology (apiculate, with a large oil droplet), suggested an affiliation of this genus with either Morchellaceae or Discinaceae (Kimbrough 1994, Li 1997). Cylindrical Woronin bodies and multinucleate ascospores have also been observed in Imaia (Kovács et al. 2008), and the smooth, ellipsoidal spores of Kalapuya resemble those of Morchella, despite being much larger in size (Trappe et al. 2010).

The various taxa of hypogeous Morchellaceae also share some features in common. Species of Fischerula, Imaia, Kalapuya, and Leucangium all have a peridium composed of nearly isodiametric cells that are sometimes raised in warts or patches. Species of Kalapuya, Imaia, and Leucangium all have a mottled, blotchy gleba with darker patches of ascogenous tissue haphazardly distributed among sterile veins (although the gleba in Fischerula species is more clearly marbled by sterile veins). Despite similarities in some morphological features, the different genera of hypogeous Morchellaceae have spores that are quite distinct from one another. Leucangium species have smooth, golden yellow, fusiform-apiculate spores with a large oil droplet; Fischerula species have brown black, ellipsoid spores with agglutinated spines or conical warts; the monospecific *Imaia* (*I. gigantea*) has spores that are globose, yellowish, and covered by a mucilaginous secondary wall (Kovács et al. 2008), and monospecific Kalapuya (K. brunnea) has smooth, ambercoloured, ellipsoid spores that contain a large oil droplet (Trappe et al. 2010). Some of the key morphological features of the four hypogeous Morchellaceae genera are shown in Fig. 1.

As with many truffle-forming fungi, the evolutionary relationships between hypogeous *Morchellaceae* genera and their epigeous relatives have been more conclusively supported through molecular analyses, although the exact placement of these genera and the monophyly of the truffle taxa have not been definitively resolved. O'Donnell *et al.* (1997) were the first to include hypogeous *Morchellaceae* in a molecular phylogenetic analysis. They concluded that *Leucangium* and *Fischerula* were closely related to the epigeous *Morchellaceae* but were unable to confidently resolve the exact relationship between these genera (O'Donnell *et al.* 1997). Based on a larger dataset Hansen & Pfister (2006) resolved *Leucangium* and *Fischerula* as the sister clade to

all other epigeous *Morchellaceae*, although this analysis included relatively few *Morchellaceae* taxa. Later analysis of 18S sequences of *Fischerula*, *Leucangium*, and the newly erected genus *Imaia* placed all the hypogeous genera within *Morchellaceae* (Kovács *et al.* 2008). A subsequent analysis of LSU and *tef1* sequences of hypogeous *Morchellaceae*, including the new genus *Kalapuya*, supported the placement of all four hypogeous genera within *Morchellaceae* (Trappe *et al.* 2010). Even then, the evolutionary relationships between the *Morchellaceae* genera were not well supported and the question of a single or multiple evolutionary transitions of fruiting bodies to a truffle form remained unresolved.

There are also unresolved questions regarding the trophic ecology of Morchellaceae. Several different trophic strategies have been reported for different Morchellaceae genera, including saprotrophic, endophytic, and ectomycorrhizal (ECM). Morchella species have received the most study due to interest in their cultivation. Morchella rufobrunnea and various 'black morel' species such as M. sextelata have been cultivated successfully in the absence of ECM hosts, suggesting a saprotrophic habit as their main mode of carbon acquisition (Ower 1982, Masaphy 2010, Narimatsu et al. 2023, Liu et al. 2023). Further evidence of saprotrophic ecology for certain Morchella species has been demonstrated through an isotopic study that reported the carbon in fireassociated Morchella species collected in Oregon and Alaska was not derived from recent photosynthate (Hobbie et al. 2016). Earlier studies reported Hartig-net-like intracellular colonization of root tissue by Morchella in pure culture synthesis experiments (Dahlstrom et al. 2000), and a patent for Morchella cultivation described axenic colonization of root systems of various trees inoculated with Morchella spores, including both ECM hosts and non-ECM hosts (Miller 2005). However, root colonization and even Hartig-net-like structures have also been synthesized in pure culture studies with several definitively saprotrophic fungi, so axenic root colonization may not be evidence of functional ECM trophic ecology (Vasiliauskas et al. 2007, Smith et al. 2017). Further, there are no reports of naturally occurring Morchella ECM root tips, indicating that ectomycorrhizal symbiosis is likely not an important aspect of Morchella ecology. Another study found abundant M. elata hyphae and sclerotia encasing multiple ECM root tips formed by other (unidentified) ECM fungi on Picea abies. While there was no direct evidence of parasitism (e.g., no haustoria) or interaction between the M. elata and the ECM fungi, the abundant hyphae and sclerotial tissue suggested some kind of specific interaction between M. elata and ECM root tips colonized by other fungi (Buscot 1994). Additionally, some *Morchella* species seem to regularly occur as endophytes within roots of healthy plants and lichens, although the ecological and biological implications of these interactions remain unclear (Baynes et al. 2012, Baroni et al. 2018, Healy et al. 2022). Isotopic evidence indicates species of Disciotis and Verpa may be saprotrophic, but these genera have not been extensively studied (Hobbie et al. 2001). Species of these genera have not been detected as ECM in roots or as endophytes of living plant tissue (Healy et al. 2022).

As with epigeous *Morchellaceae*, the primary focus in understanding the ecology of the hypogeous *Morchellaceae* has been directed at the most economically valuable species, *Leucangium* cf. *carthusianum*, from northwestern



Fig. 1. Epigeous and hypogeous *Morchellaceae*. **A.** *Fischerula subcaulis*. **B.** *F. macrospora*. **C.** *Fischerula* sp. asexual morph. **D, E.** *Fischerula* sp. asexual morph stained in Congo red and viewed in DIC, showing (D) typical arrangement of hyphae and spores and (E) conidiophore with scars where previous spores have been produced. **F.** *Leucangium carthusianum*. **G.** *Kalapuya brunnea* ascocarp and (**H**) ascospores (viewed in DIC). **I, J.** *Imaia gigantea*. Scale bars: A, B, F–I, J = 1 cm; C = 1 mm; D, E = 10 μm; H = 20 μm.

North America. Numerous authors have suggested that this species has an ECM association with Pseudotsuga menziesii (Douglas-fir), a common canopy species in the wetter portions of western North America (Hobbie et al. 2001, Trappe et al. 2009, Lefevre 2012). Pseudotsuga menziesii is also a widely cultivated timber tree and widespread evenaged stands of pure P. menziesii are common in this region. North American Leucangium cf. carthusianum is most often found in young (10-50-yr-old) P. menziesii timber stands or other areas with a history of recent disturbance, such as afforested pastureland (Pilz et al. 2009, Trappe et al. 2009). Palfner & Agerer (1998) included a description of putative Leucangium ECM root tips of P. menziesii, which included a morphological description and colour photograph. However, no molecular data were obtained in that study to confirm the association. In 2016, a Leucangium ITS rDNA sequence was generated from pooled root tip samples in a study of ECM fungal communities of P. menziesii in the Pacific Northwestern USA, but due to the pooled sampling strategy, no matching individual root tips were available for further verification (Benucci et al. 2016). Similarly, a single ECM root tip ITS sequence of a unique Fischerula species was reported from an Abies religiosa stand in Mexico (Oros-Ortega et al. 2017) and a single ITS sequence of F. macrospora from a root tip was obtained from a Populus stand in Austria (Krpata et al. 2008). Despite a general association with mixed or Pinaceaedominated habitats, there have been no reports of ECM root tips from species of Kalapuya or Imaia. A stable isotope analysis showing that δ^{13} C and δ^{15} N values from samples of Fischerula and Leucangium clustered with those of other known ECM taxa further supported the hypothesis of putative ECM ecology (Hobbie et al. 2001). Multiple attempts to grow hypogeous Morchellaceae taxa in axenic culture on various media formulations have been unsuccessful (Lemmond et al. unpublished data), and attempts to directly inoculate P. menziesii seedlings with Leucangium ascospores were also unsuccessful (G. Bonito, unpubl. data). The total accumulated evidence in this group of fungi led Tedersoo & Smith (2013) to consider the four hypogeous genera of Morchellaceae as the /leucangium ECM clade. However, evidence of the ECM trophic mode is still tenuous.

As with other truffle fungi, species of hypogeous Morchellaceae fruit either partially or entirely belowground and lack the ability to actively discharge their ascospores. The intense aromas of some Morchellaceae truffles that are responsible for their culinary appeal to humans exemplifies a notable trait of many truffle fungi: the use of strong odours to attract animal dispersers. It has therefore been assumed that animal mycophagy is an important vehicle for spore dispersal. In Pacific Northwestern USA, researchers detected Morchellaceae truffles in the diets of many mycophagous mammals, such as the northern flying squirrel (Glaucomys sabrinus), chipmunks (Tamias and Neotamias spp.) and voles (Clethrionomys spp.) (Trappe 1975, Trappe et al. 2009, Sultaire et al. 2023). Leucangium spores have also been detected in rodent scat from northeastern North America (USA and Canada) (Cloutier et al. 2019, Borgmann-Winter et al. 2023). Another recent study of rodent mycophagy detected Leucangium spores in scat samples from Apodemus flavicollis, A. agrarius and Clethrionomys glareolus in the Carpathian Mountains in central Europe (Komur et al. 2021).

Despite the culinary appeal and cultural importance of some North American Morchellaceae truffles, there are many open questions about the evolution, ecology, and systematics of these fungi, including unknown aspects about their species diversity, trophic ecology, and transition to a truffle morphology. The goal of this study was to provide a modern overview of hypogeous Morchellaceae based on newly generated morphological, molecular, and isotopic evidence. We employed a combination of amplicon and genome sequencing from fungarium collections and new specimens along with environmental DNA sequences to assess the diversity of these fungi. Although the focus of this work is primarily on taxa from North America, we also included sequence data from both European and Asian specimens. We hypothesized that new phylogenomic and isotopic data would support a single evolutionary transition from saprotrophy to the ECM trophic mode within Morchellaceae, and that this would be correlated with a single evolutionary transition to the truffle-like morphology. We also hypothesized that additional DNA sequence data would uncover novel diversity of unrecognized species.

MATERIALS AND METHODS

Field collections and fungarium specimens

Specimens were obtained from herbaria and personal collections from Canada France, Greece, Italy, Japan, Poland, and the United States. Fresh specimens of Fischerula, Kalapuya and Leucangium were obtained from Oregon and Washington, USA, with the assistance of trained dogs. Fresh Imaia samples were collected from North Carolina and Tennessee through field surveys without dog assistance. Samples from mycophagous rodent scat were obtained from Second College Grant in Coos County, New Hampshire, USA during 2018-2020 and include one dried composite scat sample from vole and mouse species (Clethrionomys gapperi, Peromyscus maniculatus, and Napaeozapus insignis) (Stephens 2020, unpubl. data) and one sample of eastern chipmunk (Tamias striatus) scat containing spores stored in ethanol (Borgmann-Winter et al. 2023). Specimens from new collections were deposited in the Florida Natural History Museum Fungarium at the University of Florida (FLAS-F). Herbarium numbers, GenBank accession information, and other data of specimens included in this analysis are provided in Table S1.

Morphological analysis of fungi specimens

Specimens were sectioned by hand with a razor blade and mounted in deionized water, 3 % KOH, Congo red, or Melzer's reagent for observation of microscopic features. Morphological analyses generally followed the methods and terminology of Healy *et al.* (2023). Spore samples from mycophagous rodent scat samples were mounted in deionized (DI) water. Measurements of microscopic features were made in DI water or 3 % KOH using a Zeiss Axio Imager A2 compound microscope (Carl Zeiss, Oberkochen, Germany). Bright-field and differential interference contrast (DIC) images were captured with an Axiocam 305 camera using Zen Pro v. 3.1

software (Carl Zeiss, Oberkochen, Germany). Measurements were performed on CZI images with Zen Pro v. 3.1. In some cases, multiple images were stacked and blended to combine focal planes using Photoshop CS5 v. 12.1 (Adobe Systems Incorporated, San Jose, CA, USA). For mature specimens, we measured ascospores, ascospore length-to-width ratio (Q), asci, excipular features, and dimensions of excipular hairs (when present). Minimum, maximum, mean, and standard deviations (as "mean \pm 1 s.d.") are reported for asci, ascospores, and excipular cell dimensions. Ascopores of *Imaia* were measured inclusive of the secondary wall, which can appear as minute ornamentation.

Molecular methods

Fungal DNA from ECM root tips and fresh truffle specimens used for rDNA barcoding was extracted using an alkaline quick extraction method (Vandepol et al. 2020). For all other samples (i.e. samples used in multi-locus analysis or genome sequencing), genomic DNA was extracted using modified CTAB extraction methods (Gardes & Bruns 1993, Fauchery et al. 2018) or a modified glassmilk extraction technique (Lindner & Banik 2009).

The nuclear rDNA internal transcribed spacer (ITS) region ITS1-5.8S-ITS2 and nuclear large subunit (LSU) were PCR-amplified using the primer pairs ITS1f-ITS4 (White et al. 1990, Gardes & Bruns 1993) and LROR-LR5 (Hopple & Vilgalys 1994) following the protocols of Gardes & Bruns (1993). The PCR amplification of the translation elongation factor 1-alpha (tef1) was performed with primer pairs EF1-1018F/1620R (Stielow et al. 2015), EF1-983F/1567R and EF1-1577F and EF1-2218R (Rehner & Buckley 2005) using a modified touchdown PCR protocol with an initial annealing temperature of 51 °C dropping by 0.2 °C/cycle, for 30 cycles. The 5-7 and 7-11 regions of the second largest subunit of RNA polymerase II (rpb2) were amplified using the fungalspecific primer sets fRPB2-5f/7cR and fRPB2-7cF/11aR and protocols of Liu et al. (1999). Amplification of Leucangium rDNA from mycophagous rodent scat samples was performed using two overlapping sets of custom Leucangium-specific PCR primers for the ITS1-5.8S-ITS2 and partial LSU region (LeucITS_1f: 5'-GCGGAAGGATCATTACAACG-3', LeucITS 1r: 5'-GTTCTGAAGGACTCTGGGGC-3', Leuc_ITSLSU_2f: 5'-GCCCAGAGTCCTTCAGAAC-3', Leuc_ITSLSU_2r: 5'-ATTACGCCAGCATCCTAGCC-3'), and another set of Leucangium-specific PCR primers for a short fragment of the tef1 region (LeucTEF-2f: 5'-ACCAAGGCCGGAAAGTCTTC-3', LeucTEF-2r: 5'-TGAATTTGGGGGTTGCCTCA-3'). These primers were designed using the primer design tools in Geneious v. 2020.2.4 (Auckland, New Zealand) on an alignment of sequences of Leucangium with other Morchellaceae fungi as outgroups to exclude. Primers were tested with template DNA of Leucangium, Kalapuya, and Imaia for specificity with Leucangium. PCR conditions for Leucangium primers used a standard ITS PCR protocol (White et al. 1990) modified to have an initial annealing temperature of 57 °C for both ribosomal primer pairs and 60 °C for tef1 primers, decreasing -0.1 °C/cycle over 35 cycles for all primer sets. All PCR products were visualized on 1.5 % agarose gels, enzymatically cleaned with exonuclease 1 and alkaline

phosphatase (Glenn & Schable 2005) and Sanger sequenced bidirectionally with the same primers by Eurofins Genomics (Louisville, KY, USA). GenBank accession numbers of all newly generated sequences are provided in Table S1.

Genome sequencing and assembly

Genomic DNA for genome sequencing was visualized on 1.5 % agarose gels for quality and concentration, checked for A260 and A280 ratios on a Nanodrop spectrophotometer (ThermoFisher Scientific, Waltham, MA, USA), and quantified on a Qubit fluorometer (ThermoFisher Scientific, Waltham, MA, USA) using the dsDNA HS assay kit. DNA extractions were sent to the Michigan State University (MSU) Genomics Core (East Lansing, MI, USA) for further quality control, library preparation and 150 bp paired-end sequencing on the Illumina Novaseq 6000 platform (Illumina, San Diego, CA, USA).

Genome assemblies were conducted with a custom bioinformatic pipeline modeled after the Automatic Assembly for the Fungi (AAFTF) pipeline (Stajich & Palmer 2023). All analyses were implemented on the University of Florida HiPerGator supercomputer cluster. Raw reads were trimmed of adapters and low-quality sequences and filtered using the AAFTF v. 0.4.1 tools aaftf-trim and aaftf-filter. Trimmed and filtered reads were normalized to 100X coverage using the BBMap v. 38.90 bbnorm function (Bushnell 2014). Normalized reads were assembled de novo using the SPAdes assembler v. 3.15.3 (Prjibelski et al. 2020). After discarding all contigs shorter than 1000 bp, resulting assembly contigs were screened for non-target contaminants using the NCBI Foreign Contaminant Screening tool (FCS-GX) (Astashyn et al. 2024). Contigs identified as originating from non-target organisms by FCS-GX were removed from the assemblies. Cleaned genome assemblies were then filtered for duplicate contigs using the aaftf-rmdup tool. Resulting assemblies were polished using the POLCA tool from the MaSuRCA assembler package (Zimin et al. 2013). Polished genomes were evaluated for completeness using the BUSCO package and the Ascomycota database (Simão et al. 2015).

To ensure that non-target contigs were adequately removed from assemblies, a second screening of genome assemblies was performed using BlobTools2 blobtoolkit v. 4.3.5 (Challis et al. 2020) to visualize the distribution of taxonomic categorization, GC content, and coverage of all contigs present in each assembly. Input data to BlobTools2 included taxonomic match and match alignment score of each contig by FCS-GX, Ascomycota BUSCO gene information, contig GC content, and contig coverage. Coverage was calculated by aligning reads used in assembly to the polished genome with minimap2 v. 2.28-r1209 (Li 2018), sorting the aligned reads into a BAM file with SAMtools v. 1.20 (Danecek et al. 2021), and calculating coverage with the pileup. sh function in the BBMap (v. 38.90) suite. Blob plots were generated from these data and filtered manually to exclude potential non-target contigs, low coverage contigs, and contigs with anomalous GC content. Taxonomic assignments were based on the 'bestsum' method in BlobTools2. This approach generates a taxonomic assignment for each contig based on the highest alignment scores computed by FCS-GX. Contigs were assessed at the taxonomic rank of class, and all contigs assigned a match other than Pezizomycetes



were excluded. Contigs that were not assigned any matches in the FCS-GX database ('no-hit') were only excluded if they contained anomalous GC content or low coverage.

Filtered assemblies were re-evaluated with the *Ascomycota* odb-10 BUSCO database. Summary statistics for the filtered assemblies were generated with the assembly-stats package v. 1.0.1 (Hunt 2017) and are provided in Table S2. Genomes with BUSCO completeness scores below 80 % were excluded from subsequent analyses. Raw sequencing data as well as *de novo* genome sequences are deposited on NCBI Sequence Read Archive (SRA) under the BioProject accession PRJNA1112361. Previously published genomes of *Morchella snyderi* (Steindorff *et al.* 2022) and *M. importuna* (Murat *et al.* 2018, Tan *et al.* 2019) were downloaded from the US Joint Genome Institute (https://genome.jgi.doe.gov).

Phylogenetic analyses

In addition to generating sequences as described above, reference ITS, LSU, *tef1*, and *rpb2* sequences for *Morchellaceae* isolates were obtained from GenBank. Additional sequences from environmental metabarcoding projects were obtained from the GlobalFungi database (https://globalfungi.com) (Větrovský *et al.* 2020) using *Morchellaceae* genera names as queries. Reference sequences used in phylogenetic analyses are reported in Table S1.

We conducted four different phylogenetic analyses:

1) ITS analyses of *Fischerula* and *Leucangium*, including sequences from truffle specimens, environmental samples, anamorphic spore mats, rodent fecal samples, and ECM root tips 2) an ITS+LSU analysis of *Imaia* that includes all named taxa and putative new taxa; 3) a multi-locus analysis of LSU, *tef1*, and *rpb2* sequences from epigeous and hypogeous *Morchellaceae* genera and *Discinaceae* outgroups; and 4) phylogenomic analysis of *Morchellaceae* and *Discinaceae* outgroup genome sequences, including representatives from all *Morchellaceae* genera. Preliminary analyses supported the monophyly of all available and newly generated *K. brunnea* sequences and did not indicate the presence of cryptic taxa in this monospecific genus, so we did not include an analysis of *Kalapuya* ITS sequences (data not shown).

Analyses of ITS (Fischerula, Leucangium) or ITS+LSU sequences (Imaia) were conducted separately by genus because of the high level of nucleotide divergence in ITS sequences between genera. An ITS+LSU analysis was chosen for Imaia to include the most robust possible analysis of all existing and proposed species and combinations. since we were unable to obtain tef1 or rpb2 sequences from any I. gigantea specimens from Japan. For each analysis, sequences were aligned with MUSCLE v. 3.8.425 (Edgar 2004) using default settings in Geneious v. 2020.2.4 (Auckland, New Zealand), with ambiguously aligned regions excluded from further analysis using GBlocks (Talavera et al. 2007) with the following settings: minimum sequence for flank position = 55 %, maximum contiguous non-conserved positions = 8, minimum block length = 5, and gaps allowed in half of final blocks. Phylogenetic analysis for each alignment was conducted with maximum likelihood (ML) using RAxML-NG on the CIPRES science portal (Miller et al. 2010) and the GTR+G model of nucleotide substitution with 1000 bootstrap replicates. The resulting trees were visualized and midpoint rooted in FigTree v. 1.4.4 (Rambaut 2018).

Multilocus phylogenetic analyses based on LSU, tef1, and rpb2 were performed to provide a more robust assessment of monophyly of the hypogeous Morchellaceae and to evaluate gene tree concordance among three commonly used phylogenetic markers. This analysis also allowed the inclusion of certain key samples and species with sequences for some loci but for which genome data were unavailable. For this analysis, representative LSU, tef1, and rpb2 sequences were compiled for all Morchellaceae genera using several Discinaceae genera (Discina, Gyromitra, Hydnotrya, Maublancomyces) as outgroups. All specimens included in the multilocus analysis were represented by at least two of three loci, and specimens with missing data were only included if they were the only representatives of a species or geographic region of particular importance (e.g. L. purpureum sequences from Asia). Alignments were performed with the same software as above and were manually trimmed so that the ends of each alignment contained sites represented by at least 75 % of sequences. Three introns were manually removed from the tef1 alignment and one intron was removed from the rpb2 alignment. Ambiguously aligned regions of the LSU alignment were removed using GBlocks as described above. Appropriate models of substitution were determined using JModelTest v. 2.1.1 (Darriba et al. 2012). The ML phylogenetic inference was performed for each alignment separately and resulting trees were checked for conflict. Alignments were then concatenated in Geneious, and the resulting concatenated alignment was analysed using RAxML-NG with separate models selected for each gene partition. Bayesian phylogenetic inference was also performed on the concatenated and partitioned alignment, using MrBayes v. 3.2.7 implemented on the University of Florida Research Computing HiPerGator supercomputing cluster. The MrBayes analysis employed two runs of four chains each, running for 20 M generations and sampled every 1000th generation, with the first 25 % of samples discarded as burn-in. Stationarity was evaluated using the "convenience" package in R (Fabreti & Höhna 2022). Posterior probabilities ≥ .95 and bootstrap values ≥ 70 % were considered as significant support. Topology and branch support from the Bayesian analysis was compared to the ML analysis and checked for supported conflicts.

Phylogenomic analysis was conducted to provide the most robust assessment of the evolutionary relationship between hypogeous and epigeous Morchellaceae taxa and the sister family Discinaceae. Initial phylogenomic analyses were performed using the Universal Fungal Core Genome (UFCG) pipeline (Kim et al. 2023), which extracts sequences of 61 'core gene' sequences from candidate assemblies when the genes are present and not duplicated. Marker genes represented by fewer than 50 % of samples were excluded from subsequent analyses, resulting in a final dataset of 52 core genes used for tree building. Phylogenetic analysis of the concatenated dataset was conducted with IQ-TREE implemented in the UFCG pipeline. To compare the results derived from the UFCG core genes compared to other marker sets, we also performed phylogenomic analyses on a filtered set of Ascomycota BUSCO loci. Single-copy BUSCO genes were extracted from all genomes using the 'Ascomycota-odb10' dataset and aligned with MAFFT v. 7.520 using the 'localpair' mode. Alignments were trimmed of ambiguously aligned regions with TrimAl v. 1.4.1(CapellaGutiérrez et al. 2009) using the 'gappyout' mode. Trimmed alignments with less than 50 % sample representation and fewer than 100 amino acids were removed, resulting in a dataset of 1497 loci. Preliminary ML trees were made with IQ-TREE v. 2.2.2.7 (Minh et al. 2020) using the 'TESTMERGE' option to determine optimal amino acid evolution models (Kalyaanamoorthy et al. 2018) and 10000 ultrafast bootstraps (Hoang et al. 2018). Trees were then pruned of potential paralogs using TreeShrink v. 1.3.9 to remove individual branches that increased the overall tree diameter by more than 10 % (Mai et al. 2018). A summary coalescent tree was then generated from the trimmed trees with ASTRAL-4 implemented by ASTER v. 1.16 (Zhang et al. 2022), with branches annotated with quartet frequencies. Branch lengths of the species tree were then estimated by ML analysis of the partitioned concatenated amino acid alignment in IQ-TREE using models of substitution estimated in the preliminary treebuilding step. All analyses were performed on the University of Florida HiPerGator. Trees were visualized and re-rooted with Discinaceae as the outgroup in FigTree v. 1.4.4 and annotated with Adobe Illustrator v. 25.11 (Adobe Systems Incorporated, San Jose, CA, USA).

Ectomycorrhizal root sampling and imaging

To assess the trophic mode of Morchellaceae truffles, we sampled ECM root tips beneath fresh truffle collections made in natural habitats. We collected fresh, healthy ECM roots in soil adjacent to Fischerula (n = 1), Imaia (n = 4), Kalapuya (n = 2), and Leucangium (n = 24) collections. Soil was collected using a hand trowel, placed in clean plastic bags, and stored on ice until processing. Soil was sieved through a 1 mm screen and root samples were gently rinsed several times in tap water to remove soil particles prior to morphological examination. Some cleaned ECM root tip samples of each morphotype also were stored in 95 % ethanol for 5-10 d for transport and long-term preservation. ECM root tips were examined with a Leica MZ-16 stereomicroscope (Leica, Wetzlar, Germany) in autoclaved DI water, grouped into morphotypes, and photographed using a Zeiss Axiocam 208 camera and Zen Pro (v. 3.1) software (Carl Zeiss, Oberkochen, Germany). For each morphotype, 1–3 individual healthy, terminal ECM root tips were removed with a clean scalpel, dried of excess water with a Kimwipe, and placed individually in a tube containing 25 µL alkaline buffer for subsequent DNA extraction (Vandepol et al. 2020).

Since we found plentiful Leucangium ECM root tips of a consistent morphology and DNA sequence, we selected Leucangium root tips for imaging to visualize the ECM morphology. Root tips were fixed in 5 % formalin with 5 % acetic acid in 50 % ethanol for 24 h on a shaker set to the lowest speed. The fixed roots were rinsed in three changes of 50 % ethanol, and then gradually dehydrated in an ethanol series (50 %, 70 %, 95 %, several changes in 100 %) to absolute ethanol followed by 1:1 absolute ethanol:xylene and then several changes of xylene, with a minimum of 12 h in each solution, agitated on a shaker. The root tips were gradually infiltrated with melted Paraffin (mp of 56 °C) in a 60 °C oven, with occasional agitation over the course of seven days until the paraffin had completely displaced the xylene. Root tips were perpendicularly oriented in fresh, melted paraffin in an embedding tray and allowed to harden

overnight. Blocks of root tips were trimmed, and 8 µm thick cross-sections were cut with a Microm HM 325 (GMI, Ramsey, MN, USA) microtome and mounted on ProbeOn Plus slides (Thermo Fisher Scientific) and allowed to set overnight in a 55 °C oven. Paraffin-embedded samples were then hydrated by passing them through a dilution series for 5 min each of two washes with Histo-Clear II (National Diagnostics, Atlanta, GA, USA), two washes with 100 % ethanol, 95 % ethanol and 70 % ethanol, then placed in 10 % KOH for 10 min, and washed three times in PBS. Sections were stained for 1 h with 5 µg/mL fluorescein isothiocyanate conjugated wheat germ agglutinin (FITC-WGA) (Sigma L4895-5MG) in PBS, washed three times in PBS, and mounted in Fluormount-G (Invitrogen) on a microscope slide overlaid with a cover slip. WGA is a chitin-specific lectin and binds selectively to N-acetyl glucosamine along fungal cell walls in samples with both plant and fungal tissue (Carotenuto & Genre 2020). WGA fluorescence was visualized on a Leica DMR 020-525.024 (Leica, Wetzlar, Germany) compound microscope equipped with an Endow GFP Longpass filter (Nikon, Tokyo, Japan), with a 450-490 nm excitation wavelength. The expected emission of chitin-bound WGA is 500 nm (green). Images of samples in brightfield and fluorescence microscopy were taken at multiple focus depths with a Leica DFC450-C camera (Leica, Wetzlar, Germany) at 200× and 400× magnification. Images were integrated to reconstruct a complete, in-focus view of the entire root tip cross section using Adobe Photoshop.

Isotopic analysis

An analysis of δ^{13} C and δ^{15} N values of *Morchellaceae* truffles, epigeous *Morchellaceae*, and known saprotrophic and ECM fungi was conducted to further test the hypothesis of ECM trophic mode for *Morchellaceae* truffles. This analysis employed existing data from a wide array of fungal groups of known trophic modes based on Mayor *et al.* (2009) as a training dataset for a quadratic discriminant analysis (QDA) model (Birkebak *et al.* 2013). This model was used to predict the trophic status (either ECM or saprotrophic) of a test dataset composed of newly generated δ^{13} C and δ^{15N} values as well as values for *Morchellaceae* taxa from other sources (Hobbie *et al.* 2001). Model predictions with posterior probability values > 0.8 were considered strongly supported (Birkebak *et al.* 2013).

Fresh specimens of *Imaia* (n = 7), *Kalapuya* (n = 2) and *Leucangium* (n = 12) were collected in several sampling trips between July 2021 and April 2022. Where available, we also collected co-occurring taxa that were known to be either ECM or saprotrophic. We also sampled several additional fresh collections of *Fischerula subcaulis*, *Morchella americana*, *M. punctipes* as well as assorted fungarium specimens of various *Morchellaceae* taxa. Fresh samples were air-dried, and all samples were homogenized with 2-mm-diam. steel balls in a MiniG-1600 shaker at maximum speed for at least 60 s, lyophilized, and stored in 1.5 mL tubes until further analysis.

Isotopic and compositional properties of *Leucangium*, *Kalapuya*, *Fischerula* samples were measured at the Light Stable Isotope Mass Spectrometry Lab at the University of Florida (Gainesville, FL, USA). For each sample, %C, %N, δ^{13} C, and δ^{15} N were measured. All carbon isotopic results

were expressed in standard delta notation (δ^{13} C) relative to Vienna Peedee Belemnite. All nitrogen isotopic results are expressed in standard delta notation ($\delta^{15}N$) relative to air. Morchella and Imaia specimens were measured at the MSU Stable Isotope Core facility (East Lansing, MI, USA). For these samples, tissues were homogenized in a TissueLyser II (QIAGEN) using steel beads, acidified with 1.5 to 3 mL of 1 N HCl, dried in beakers at 37 °C and weighed for biomass. Isotopic composition of the samples %C, %N, δ¹3C, and δ¹⁵N were determined using a Eurovector (EuroEA3000) elemental analyzer coupled with an Elementar Vario Isotope cube following a standard protocol (Fry 2007). δ13C and δ15N values generated in this study, along with sample metadata, are provided in Supplemental Table S3. The QDA model was calculated in RStudio (2023.06.2+561) using R version 4.3.1 (R Core Team, 2023) using the gda function in the MASS package (Venables & Ripley 2002). Data were visualized in R using the ggplot2 package (Wickham 2016).

RESULTS

Phylogenetic and phylogenomic analyses

A total of 139 ITS sequences, 104 LSU sequences, 38 tef1 sequences, and 9 rpb2 sequences were generated for this study; 35 additional sequences of tef1 and rpb2 were extracted from genome assemblies generated during this study. De novo genome assemblies were completed for 34 Morchellaceae and five Discinaceae samples. Of these, seven Morchellaceae assemblies with BUSCO completeness scores < 80 % were excluded from further analysis. A complete list of GenBank accession numbers and corresponding sample metadata for samples used in this study is provided in Table S1. Genome assembly summary statistics and BUSCO scores are provided in Table S2.

Alignments used for the ITS analyses consisted of 17 sequences of 772 characters for *Fischerula*, 19 sequences of 851 characters for *Imaia*, and 98 sequences of 771 characters for *Leucangium*. Each ITS analysis used the GTR+G model of nucleotide evolution. Alignment characteristics and models of nucleotide evolution selected for the multilocus phylogenetic analysis were as follows: TRN+I+G for the LSU alignment (42 sequences of 852 characters), SYM+G for the *tef1* alignment (42 sequences of 999 characters), SYM+I+G for the *rpb2* alignment (38 sequences of 812 characters). Individual gene trees were checked for supported conflicts prior to concatenation. The concatenated multilocus analysis was rooted with sequences of *Gyromitra esculenta* and *Hydnotrya cubispora* from the sister family *Discinaceae*.

Phylogenetic analyses indicated the presence of undescribed genetic diversity in *Fischerula*, *Imaia*, and *Leucangium* (Figs. 2–4). The ITS analysis of *Fischerula* suggested significant diversity within specimens identified as *F. macrospora*, and sequences from a *Populus* ECM root tip clustered close to F. macrospora specimens. Further work is needed with European collections to evaluate whether these represent more than one species. The analysis also revealed undescribed *Fischerula* diversity in North America, with at least two well-supported and distinct lineages recovered, in addition to *F. subcaulis* from the Pacific Northwestern USA. One of these lineages is known only from an *Abies religiosa*

ECM root tip collected in Estado de Mexico, Mexico (Oros-Ortega et al. 2017). The other lineage was represented by a DNA sequence from a mitotic spore mat collected in Minnesota, USA (Healy et al. 2013), the only known anamorph collection of any hypogeous Morchellaceae (Fig. 2). The ITS and LSU analyses of *Imaia* specimens resolved three strongly supported clades: Imaia gigantea from Japan, a North American clade, which we combine here as I. pachyascus comb. nov., and a North American lineage that represents a new taxon, described here as I. kuwohiensis sp. nov. Despite multiple attempts to obtain tef1 and rpb2 with standard PCR as well as Illumina sequencing and assembly of genomic DNA, these additional loci were not obtained from any I. gigantea specimens included in this analysis. As a result, a more robust multilocus analysis was not possible for I. gigantea.

The ITS, multilocus, and phylogenomic analyses recovered two strongly supported North American Leucangium clades, L. cascadiense sp. nov. and L. oneidaense sp. nov., and a third clade L. purpureum comb. et stat. nov. that is present in Asia, Europe, and North America. The ITS analysis also includes sequences of ECM root tips from Pseudotsuga that were collected adjacent to fresh truffles of L. cascadiense in western North America (Fig. 2). We confirmed ECM root tips colonized by L. cascadiense from four truffle collection sites (see below). ITS sequences from Leucangium ascospores recovered from several mycophagous mammal scat samples from eastern North America were placed within the L. purpureum clade, indicating that this geographically widespread clade occurs in eastern North America as well as western North America, even though no L. purpureum ascocarps have been reported from eastern North America (Fig. 3). Leucangium samples from Europe were distributed in two clades, these include the geographically widespread L. purpureum and another taxon that we have identified as Leucangium carthusianum based on morphological features consistent with the description of L. carthusianum (Figs 2-4). Four clades of Leucangium were detected from Asia, representing L. microspermum from Japan, L. purpureum from China, and two clades known from soil ITS2 sequences that do not correspond with any described species or ascoma collections (Fig. 2).

Both ML and Bayesian multilocus analyses LSU+tef1+rpb2 strongly supported the monophyly of the hypogeous Morchellaceae clade and monophyly of each Morchellaceae truffle genus (Fig. 3). Individual trees contained some topological differences, most of which were unsupported (Fig. S1). The rpb2 tree supported Fischerula as a sister clade to all other truffle genera, and a clade containing Kalapuya and Imaia as sister to Leucangium, while LSU and tef1 trees had varying though unsupported topologies with respect to these genera. Most species clades were supported as reciprocally monophyletic except L. cascadiense and L. purpureum, which formed marginally unsupported clades (60-69 % bootstrap support, 0.9-0.94 posterior probability) in both the LSU and rpb2 analyses. Accordingly, there was some lack of support among individual loci for the sister relationship between L. carthusianum and L. purpureum found in the concatenated multilocus and also the phylogenomic analyses (see below). All new species and combinations proposed here were supported as monophyletic by both ML and Bayesian analyses of the concatenated dataset: I.

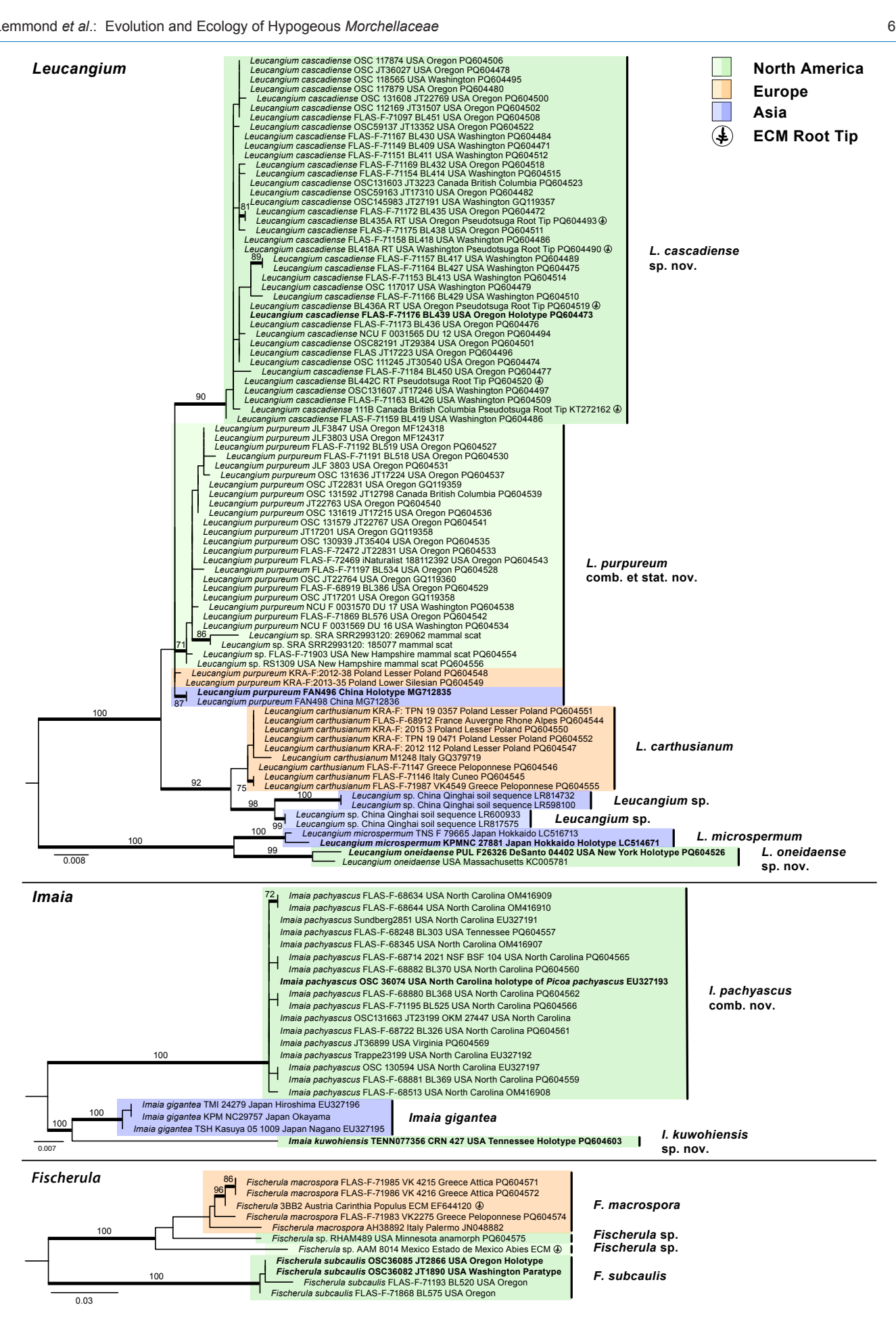


Fig. 2. Midpoint-rooted Maximum Likelihood phylogenies of ITS sequences of Leucangium and Fischerula and concatenated ITS+LSU sequences of Imaia. Branches are considered supported when bootstrap support values ≥ 70 % and are indicated with thickened lines. Type collections are indicated in **bold**. Geographic range (by continent) of each hypogeous *Morchellaceae* clade is indicated with colored shading (Asia = purple, Europe = orange, North America = green). Sequences from ectomycorrhizal (ECM) root tips are indicated by the root tip icon.

pachyascus, I. kuwohiensis, L. cascadiense, L. oneidaense, and L. purpureum.

The ML phylogenomic analysis was conducted with two datasets. The first analysis used 52 protein-coding genes identified as 'core' fungal genes by UFCG and employed the UFCG analysis pipeline. We also conducted a separate summary coalescent phylogenomic analysis with a filtered set of 1497 Ascomycota BUSCO genes, with branch lengths estimated by ML using a concatenated partitioned alignment of those loci. Both phylogenomic analyses recovered a similar topology and patterns of gene conflict in the species tree (Fig. 4). The relationship between Disciotis, Imaia, and Verpa (and their sister genera) showed significant discordance in both analyses. The monophyly of all individual Morchellaceae genera, however, were strongly supported in both analyses. The phylogenomic analysis was also congruent with the multilocus analysis in supporting the monophyly of the hypogeous Morchellaceae (supported by 82 % of BUSCO loci and 35 of 52 UFCG loci), and also the monophyly of each of the four hypogeous genera. In contrast to our LSU+*tef1*+*rpb2* analysis, the phylogenomic analysis placed *Imaia* as the sister genus to *Leucangium*, rather than the clade containing *Imaia* and *Kalapuya* as sister to *Leucangium* (Fig. 3), though this topology was not well supported (i.e. supported by only 45 % of BUSCO loci and 20 of 52 of UFCG loci) (Fig. 4). *Imaia kuwohiensis*, *I. pachyascus*, *L. cascadiense*, *L. oneidensis*, and *L. purpureum* are all supported as monophyletic.

The monophyly of all species groups were strongly supported (i.e., by a majority of gene trees) in the phylogenomic analyses. The most discordance at the species level was observed in *L. purpureum*, where 62 % of the BUSCO loci and 34 of 52 UFCG core genes supported the primary topology, while other *Morchellaceae* truffle species clades were supported by at least 88 % of BUSCO loci and 49 of 52 UFCG loci (Fig. 4) [Note that the type of *L. purpureum* was not available for study, but the limited data of the *L. purpureum* type specimen included in our multilocus (LSU+tef1+rpb2) analysis provided no support for clades of *L. purpureum* that are specific to each continent – Fig. 3]. The monophyly of all *L. carthusianum* samples was strongly

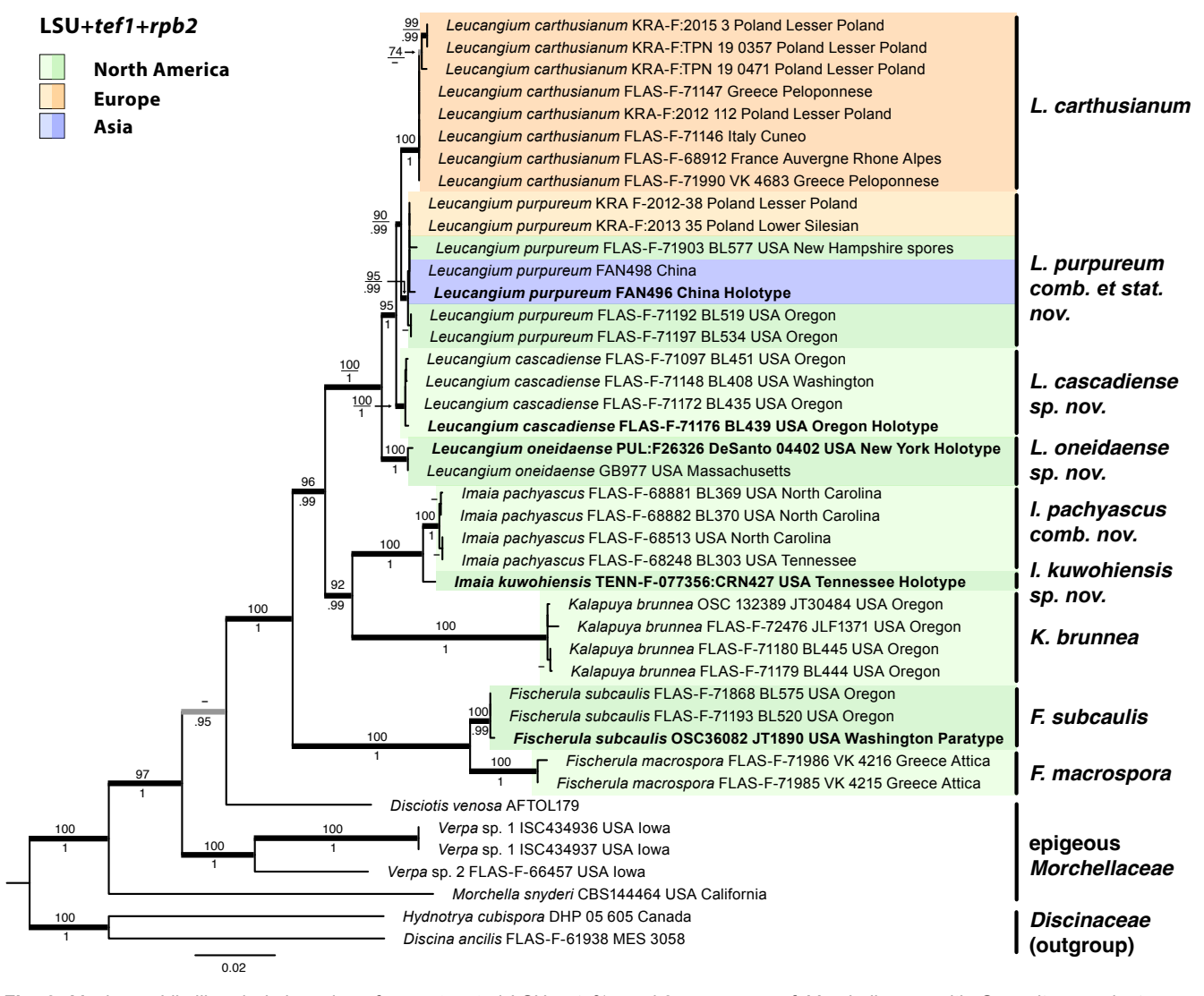
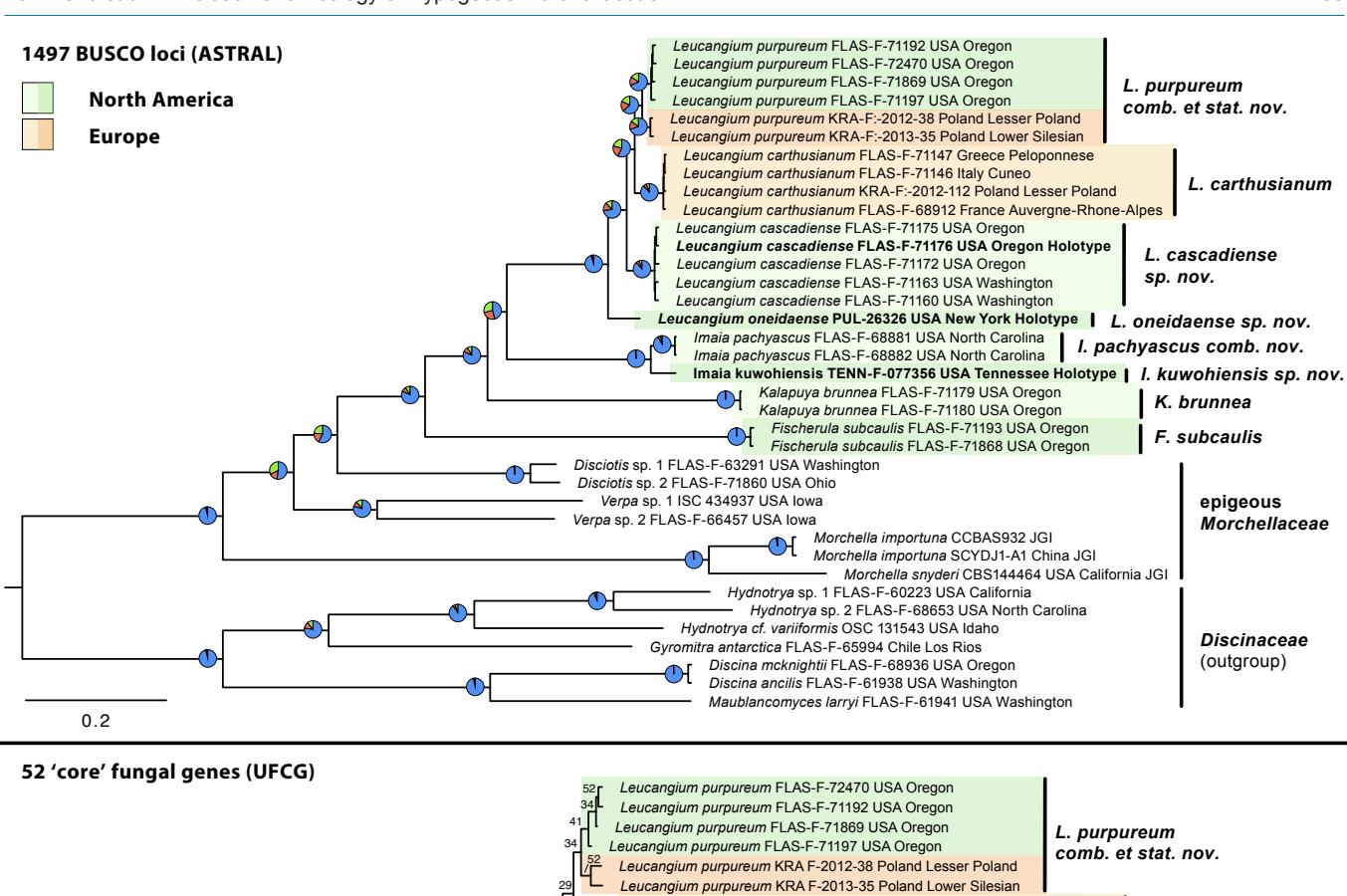


Fig. 3. Maximum Likelihood phylogenies of concatenated LSU + tef1 + rpb2 sequences of testing Morchellaceae with testing Morch



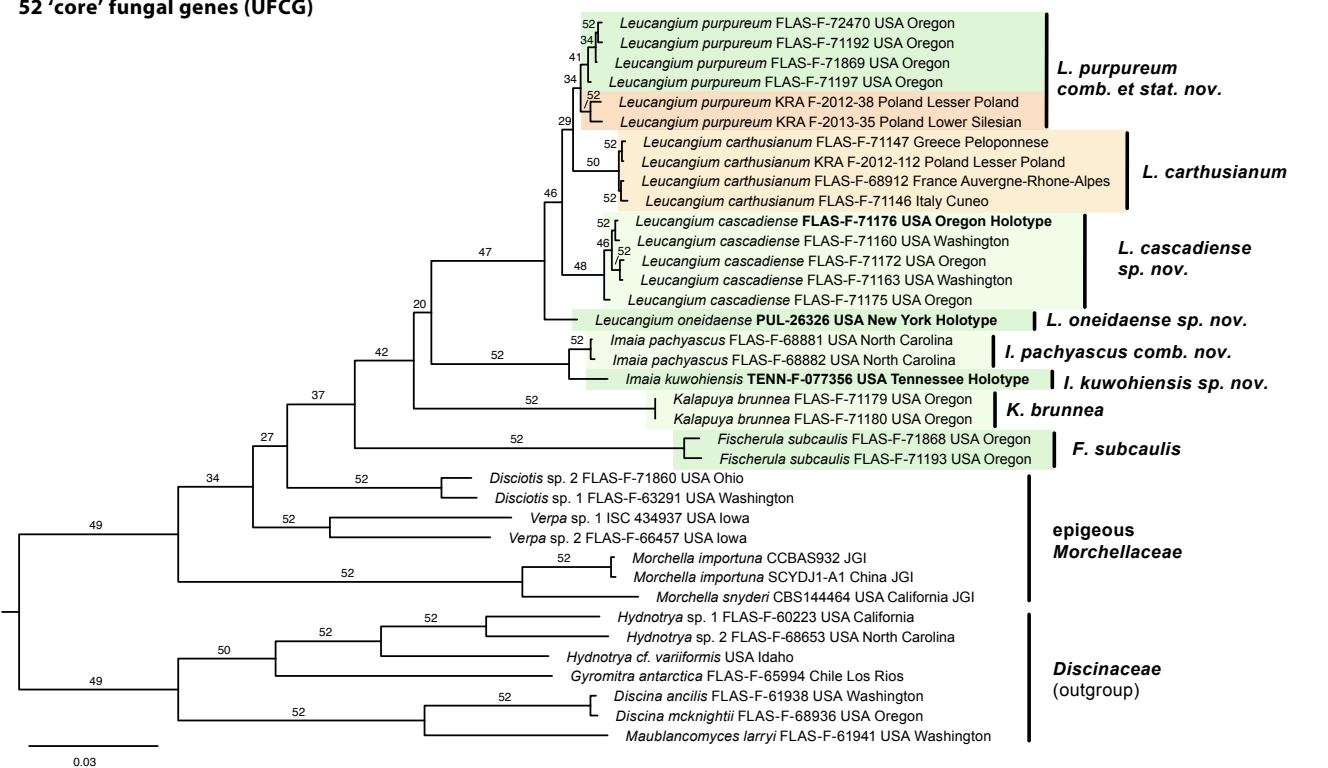


Fig. 4. Two phylogenomic analyses of genomic datasets. **Top.** Phlyogenomic species tree derived from ASTRAL coalescent analysis of Maximum Likelihood trees of 1497 Ascomycota BUSCO loci extracted from genome assemblies of *Morchellaceae* and *Discinaceae* (outgroup). Quartet values (a measure of gene tree concordance) are plotted as pie charts at most nodes, except those corresponding to terminal clades with near-zero length. The proportion of trees supporting the dominant topology are represented in blue, and the proportion of trees supporting the two alternative topologies are in red and green. **Bottom.** The ML analysis with IQ-TREE of a concatenated alignment of 52 "core" fungal genome loci identified by UFCG. The gene support index (GSI) of each node is provided as a number (e.g., a GSI of 52 indicates that all genes support the tree topology as shown). Type collections are indicated in **bold**. Geographic range (by continent) of hypogeous *Morchellaceae* specimens is indicated with colored shading (Europe = orange, North America = green).



supported in both phylogenomic analyses, although there was equivocal support (57 % of BUSCO loci, 26 of 52 UFCG loci) for the sister relationship between L. carthusianum and L. purpureum.

Ectomycorrhizal root sampling

With the aid of trained truffle dogs, we located abundant collections of L. cascadiense in forests dominated by P. menziesii. At five collection sites we extracted healthy, intact ECM roots of P. menziesii with a consistent morphology of smooth, dark-brown mantle with no emanating cystidia (Fig. 5). Analysis of ITS sequences of ECM roots placed these samples within the L. cascadiense clade, matching the ITS sequences from adjacent truffle specimens (Fig. 2). None of the ECM root tips collected near fruiting bodies of F. subcaulis, I. pachyascus, and K. brunnea matched the corresponding truffle specimens.

Several ECM root tips with L. cascadiense sequences were selected for microtome sectioning and WGA fluorescence imaging. When visualized using fluorescence microscopy, the green chitin-bound WGA fluorescence was apparent between cortical cells of the plant root and concentrated around the outside perimeter of the root cross section, forming a Hartig net (Fig. 5). The same pattern and general morphology were consistent across all samples observed.

Isotopic Analysis

The QDA model based on carbon and nitrogen stable isotope abundances predicted an ECM trophic mode for all Imaia, Fischerula, Kalapuya, and Leucangium samples analyzed, with high posterior probability (0.91-1.00) (Fig. 6). The predicted trophic status of epigeous Morchellaceae samples were less consistent. Disciotis venosa was either predicted as ECM or undetermined, depending on the specimen. Similarly, specimens of Verpa bohemica and V. conica were either predicted as saprotrophic or undetermined. Morchella punctipes was predicted as saprotrophic while M. americana was predicted as ECM, and some specimens of M. elata were predicted as saprotrophic whereas others were undetermined. Reference samples of known ECM and saprotrophic genera generated as part of this study were also tested. All samples were predicted by the QDA model to have the same trophic mode that we hypothesized based on the literature (Mayor et al. 2009, Tedersoo & Smith 2013) except that a single specimen of Entoloma holocontium, which was hypothesized to be saprotrophic but was predicted by the model to be ECM. Trophic status predictions and posterior probabilities for all tested samples used in this study are presented in Table S3.

TAXONOMY

Morphological and molecular analyses (Figs 2-4) support the establishment of two new species of Leucangium and one new Imaia species from North America as well as one new combination within Imaia and one in Leucangium. Below we provide updated descriptions of each truffle-forming genus and describe several new taxa and combinations. We also

elevate L. carthusianum var. purpureum to species rank. We also provide an overview on the taxonomy of the North American taxa of hypogeous Morchellaceae and a synopsis about what is known about each of the four genera to provide context for the proposed taxonomic changes.

TAXONOMIC OVERVIEW

Fischerula

The genus Fischerula was established by Mattirolo (1928) to accommodate F. macrospora described from Italy. Decades later, Trappe (1975) described a second Fischerula species, F. subcaulis, from northwestern North America. Fischerula subcaulis is notable for its prominent (though variable) stipecolumella, which can extend up to 1 cm outward beyond the gleba tissue or may be appressed to the exterior of the peridium (Trappe 1975) (Fig. 1). Fischerula macrospora sometimes has a small sterile base or reduced, narrow columella that bisects the gleba in cross-section, but does not project outwards as in F. subcaulis. Fischerula macrospora is found in southern Europe, among Quercus-dominated or mixed forests (Venturella et al. 2006, Alvarado et al. 2011). Fischerula subcaulis has only been found in forests dominated by P. menziesii in northwestern North America and is apparently uncommon (Trappe 1975).

Imaia

Imaia was described in 2008 to accommodate a single species, I. gigantea, which was previously described as Terfezia gigantea by Sanshi Imai in 1933 from Japan (Imai 1933, Kovács et al. 2008). Imai described T. gigantea as a semi-hypogeous fungus ranging from "walnut-sized" to 10 × 10 × 15 cm with the largest specimens weighing up to 800 g. Imaia gigantea has a slightly warted peridium that is whitish-buff in the subterranean portion but darker brown where exposed above the surface (Fig. 11, J). Imai also noted asci possessed "rather thick" walls. He placed this taxon in Terfezia due to its apparently minutely spiny ascospores and general similarity to *T. boudieri*. *Terfezia gigantea* was later reported in North America by Gilkey from a collection found in a moss-covered stream bank in Pennsylvania, USA (Gilkey 1947). Gilkey expressed her reservation about applying Imai's T. gigantea epithet since the spores in the North American collection were larger (up to 44-52 µm diameter) than the Japanese collections (up to 32-47 µm diam.). She also interpreted the spore ornamentation as "distinctly roughened" in the collection she examined, rather than "covered with minute spines" as described by Imai.

A few years later, Lange collected five "half-exposed" ascomata among Rhododendron roots in North Carolina, USA which he described as a new species, Picoa pachyascus (Lange 1956). Lange noted the very thick (< 10 µm) ascus walls and described the spores as smooth, globose, and 36-42 µm broad. Trappe & Sundberg (1977) re-examined an assortment of North American collections of P. pachyascus from the Appalachian region and synonymized P. pachyascus with T. gigantea. They determined that Lange had collected immature specimens and they observed that the ascus



Fig. 5. A–G. Ectomycorrhizal root tips of *P. menziesii* colonized by *L. cascadiense*. H. Cross section of P. menziesii root tip collected adjacent to truffle specimen FLAS-F-71172, stained with fluorescent wheat germ agglutin (WGA) (brightfield). I. The same WGA-stained root tip cross-section visualized with fluorescence microscopy, where green areas correspond to WGA fluorescence. J–M. corresponding sections seen in brightfield (J, L) and fluorescence (K, M). WGA fluorescence surrounding the root tip exterior indicates a mantle of fungal tissue, and fluorescent areas between plant cortical cells indicate a Hartig net. Scale bars: A–G = 0.5 mm; H, I = 50 μm; J–M = 10 μm.



walls became thinner in the specimens as they matured. They also noted that the ascospores only developed what they interpreted as a spiny epispore at maturity (Trappe & Sundberg 1977).

In establishing the monospecific genus *Imaia*, Kovács *et al.* (2008) treated the Japanese and North American specimens as members of the same species. Although they did not find significant morphological differences between North American and Japanese collections, they noted significant differences in SSU, ITS, and LSU sequences between specimens from the two continents. To clarify the question of spore ornamentation, they examined the spores with electron microscopy and determined that what appeared during light microscopy as minute spines are actually pits and tunnels in a thick (3–5 μm), amorphous, mucilaginous secondary wall, which they called an epispore.

Kalapuya

Kalapuya is the most recently established genus of Morchellaceae and contains a single species, K. brunnea, which is endemic to northwestern North America (Trappe et al. 2010). Kalapuya brunnea somewhat resembles Leucangium in having a peridium with low warts or rough patches and a gleba mottled with pockets of fertile tissue surrounded by sterile, undifferentiated veins. However, the peridium of K. brunnea is brown, compared to the pinkish to purple black peridium of Leucangium species. Kalapuya brunnea and Leucangium cascadiense sp. nov. co-occur in young, disturbed P. menziesii stands and both have strong fruity aromas that make these truffles prized culinary delicacies (Trappe et al. 2010).

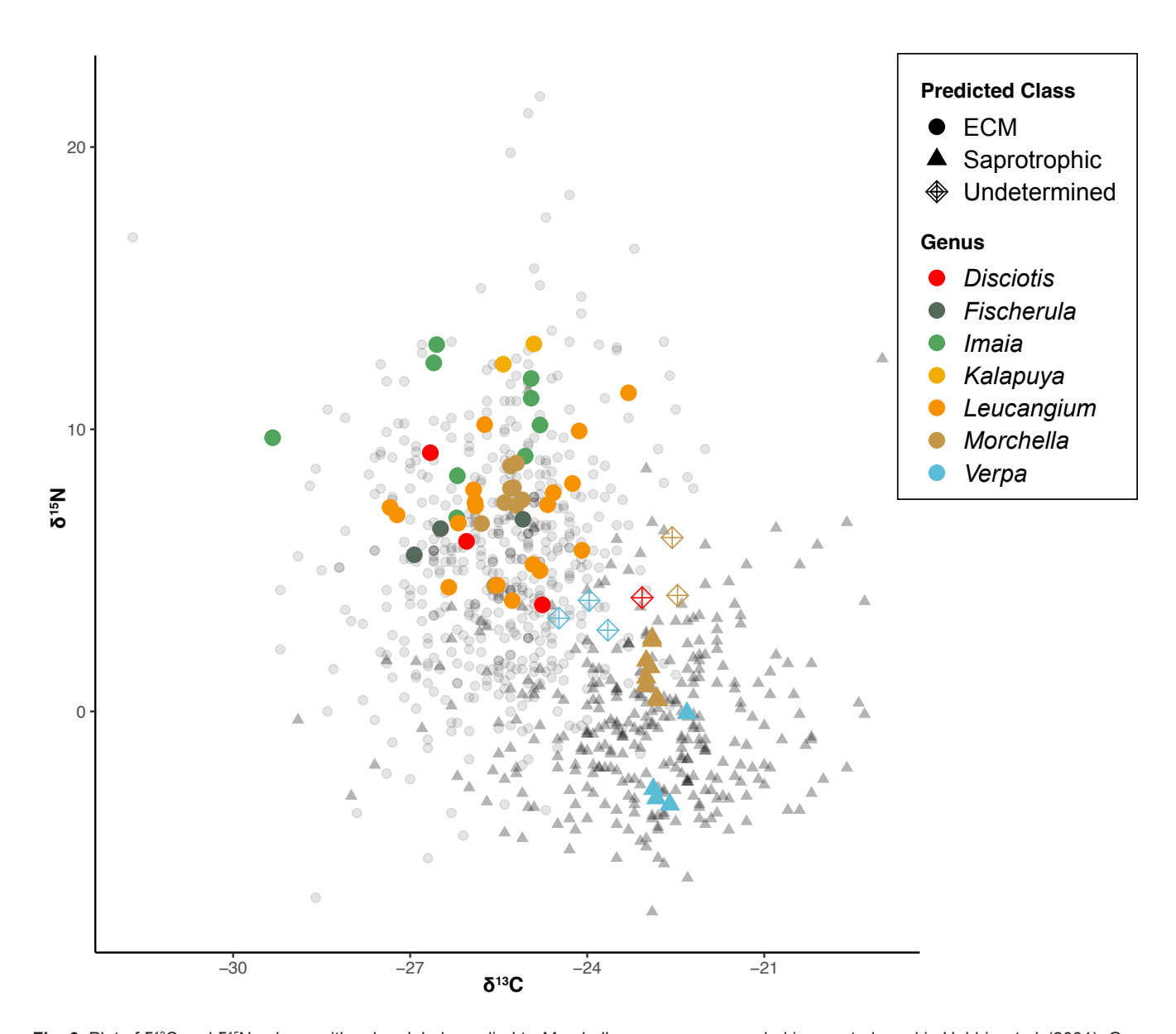


Fig. 6. Plot of δ^{13} C and δ^{15} N values, with colour labels applied to *Morchellaceae* genera sampled in our study and in Hobbie *et al.* (2001). Grey background points represent data from Mayor *et al.* (2009) of known ECM (circles) and saprotrophic (triangles) taxa used to train our quadratic discriminant analysis (QDA) model. Coloured values represent test samples and trophic group predicted by the QDA model. Model predictions were considered well-supported by posterior probability values ≥ 80 % and are indicated by solid colours; unfilled diamond shapes represent values where the model prediction was not well supported.

Leucangium

Leucangium carthusianum was originally described as Picoa carthusiana by Tulasne & Tulasne (1862) from collections of hypogeous fungi with fusiform-apiculate spores found near the Carthusian monastery in the Auvergne-Rhône-Alpes region of France. The genus Leucangium was later established by Quélet to accommodate the type species L. ophthalmosporum, also from France, which was later transferred to Picoa by Fischer (Quélet 1883, Fischer 1897). Paolocci transferred P. carthusiana to Leucangium (as L. carthusianum), noting that L. carthusianum and L. ophthalmosporum may be synonyms (Saccardo 1889). In the intervening years, there have only been infrequent collections of L. carthusianum from Europe, with specimens reported from Greece, Italy, France, and Poland. We know of no recent specimens identified as L. ophthalmosporum.

Leucangium carthusianum was first reported (as P. carthusiana) in North America from Oregon by Gilkey (1954a). Trappe (1971) proposed Leucangium as a subgenus of Picoa and formally synonymized L. ophthalmosporum and L. carthusianum. In this case, the older epithet carthusianum replaced the newer ophthalmosporum and L. carthusianum became the type species of what was then a subgenus of Picoa. Picoa (including P. subg. Leucangium) was transferred from Terfeziaceae to Balsamiaceae in 1979 (Trappe 1979). Li (1997) adopted Trappe's nomenclature in his ultrastructural study of Leucangium collections from the Pacific Northwestern USA in 1997, citing unpublished data suggesting that L. carthusianum was morphologically and genetically distinct from Picoa (Li 1997). The epithet L. carthusianum has since been applied to most Leucangium collections in North America, which primarily originate from the Pacific Northwestern USA and British Columbia, Canada (Gilkey 1954a, b, Trappe 1971, Li 1997).

Outside of North America and Europe, there have been only a few additional taxonomic works on *Leucangium*. Gilkey (1945b) rendered *Leucangium readeri* from Australia invalid after noting that the dark, lemon-shaped spores that had suggested an affiliation with *Leucangium* were in fact produced by an unidentified parasite, while the truffle itself had round ascospores inside cylindrical asci arranged in a palisade (Gilkey 1954b). More recently, one new species and one variety were described from Asia, *L. microspermum* from Japan and *Leucangium carthusianum* var. *purpureum* from China (Chen & Fan 2018, Yamamoto et al. 2020).

TAXONOMIC DESCRIPTIONS

Fischerula Mattir.

Ascomata hypogeous, subglobose to irregular, with or without stipe-columella. *Peridium* smooth to minutely scabrous-warty, often furrowed, greyish pink to yellow brown. Ectal excipulum of large, elongate to isodiametric cells with yellow to brown walls 1–3 μm thick. *Gleba* solid, of brown to purplish-black fertile tissue marbled with narrow, white to greyish yellow, palisade-lined, hypha-stuffed veins that occasionally emerge through the peridium. *Asci* 1–6(–8) spored, embedded in tramal tissue, ellipsoid to obovoid, subcylindrical or reniform, short stipitate, with multilayered walls 1–3 μm thick, inamyloid.

Ascospores ellipsoid, 49–87(–110) \times 40–73 μm including dark brown, rounded to conic warts up to 15 μm tall.

Type species: Fischerula macrospora Mattir.

Note: Description adapted from Trappe et al. (1975).

Imaia Trappe & Kovács, emend. Lemmond & M.E. Sm.

Etymology: In honour of the mycologist Sanshi Imai.

Ascomata erumpent or hypogeous, subglobose, tawny yellow to brown, often darker on exposed portions if erumpent. Peridium often cracked at maturity, verrucose, composed of subglobose to angular cells with thick walls, hyphoid hairs sparse if present. Gleba solid, composed of mottled brown pockets of fertile tissue separated by white sterile tissue. Ascospores globose to subglobose, up to 70 µm long, with a thick, mucilaginous secondary wall.

Type species: Imaia gigantea (S. Imai) Trappe & Kovács

Notes: Description based on Trappe et al. (2008) with some slight changes to reflect the verrucose peridium, occasional presence of sparse hyphoid hairs on the peridum surface, and with amended terminology to refer to the mucilaginous exterior feature of the spores. Kovács et al. (2008) describe this as an "epispore", but their TEM images show that this feature is more accurately described as a secondary wall, according to terminology used in ultrastructural studies of Pezizales spore development (Merkus 1976, Gibson & Kimbrough 1988).

Imaia pachyascus (M. Lange) Lemmond & M.E. Sm., *comb. nov.* MB 853894. Fig. 7.

Basionym: Picoa pachyascus M. Lange, Mycologia 48: 877. 1957.

Typus: **USA**, North Carolina, Macon Co., near Highlands, Sep. 1947, *M. Lange* 1917 (**holotype** of *Picoa pachyascus* Lange, C). GenBank EU327193 (ITS).

Ascomata globose to slightly lobate, 3-8 cm diam., firm, occasionally with a small mycelial tuft or sterile basal projection, but typically lacking an obvious attachment point. Erumpent or shallowly hypogeous; when erumpent, exposed peridium surface often discoloured black, particularly on the tops of the warts. Outer surface yellow brown, verrucose, with subpolygonal warts 1.5-3 mm broad by 0.25-0.75 mm tall; texture minutely scurfy, pubescent, or smooth between warts. Sparse tomentum visible in some places on excipulum, composed of linear, hyaline hyphae with yellowish walls, basal cells inflated, often encrusted with yellowish deposits. Aroma variously described by some collectors as spicysweet, rich, or fruity when mature. Immature specimens have a potato-like odour, and overmature specimens have an intense, disagreeable, and fishy aroma. Excipulum whitish, remaining whitish as the gleba matures and darkens, 0.75-4 mm thick, composed of two layers. Ectal excipulum 150-650 µm thick with cells textura globosa-angularis, outermost cells yellow brown, inflated, 20-60 µm diam., with thickened walls (2-4.5 µm), cells becoming hyaline, more angular, and



Fig. 7. *Imaia pachyascus comb. nov.* **A.** Fresh truffle sliced to show gleba. **B.** Truffle with mature gleba and thick, white peridium. **C.** Typical erumpent growth of truffle and discoloration of exposed wart apices (**D**) ascospores (viewed in DIC). **E.** Ascus with mature ascospores. **F.** Ectal excipulum tissue of the condition of the condition of truffle and discoloration of exposed wart apices (**D**) ascospores (viewed in DIC). **E.** Ascus with mature ascospores. **F.** Ectal excipulum tissue station of the condition of truffle and discoloration of exposed wart apices (**D**) ascospores (viewed in DIC). **E.** Ascus with mature ascospores. **F.** Ectal excipulum tissue (SIO) and the condition of truffle and discoloration of exposed wart apices (**D**) ascospores (viewed in DIC). **E.** Ascus with mature ascospores. **F.** Ectal excipulum tissue (SIO) and the condition of exposed wart apices (**D**) ascospores (viewed in DIC). I. Excipular hair (DIC). Scale bars: A–C = 1 cm; D = 10 μ m; E, H = 20 μ m; F, G, I = 50 μ m.

with thinner walls (1.5–2 μm) closer to medullary excipulum. Medullary excipulum 350–800 µm thick, composed of hyaline interwoven hyphae of textura intricata, cells 9-22 µm wide at septa. Gleba white to light tan throughout when young, in maturity becoming mottled with pockets of brown to chocolate brown fertile tissue separated by whitish sterile veins, hyphae 5-15 µm at septa, hyaline. Gleba texture firm, not gelatinous. Asci randomly arranged within fertile pockets in the gleba, 4-8-spored, globose to subglobose, subpyriform, obovoid, ellipsoid or irregular, in youth with a pedicel up to 28 µm long and walls up to 13 µm thick, at maturity generally lacking pedicels, (l00-)130-200 \times (80-)95-155 μ m, ascus walls 2-7 µm thick. Ascospores globose to subglobose or sub-polygonal, yellow brown at maturity with a single, large oil droplet inside, spore surface appearing finely pitted or ornamented due to mucilaginous secondary wall, 2-5 µm thick. Ascospores (including secondary wall) 31-52 (mean 43.4 ± 4) × 31–50 (mean 42.2 ± 3.8) µm, Q = 1–1.17 (mean 1.02 ± 0.02).

Distribution and Ecology: In the southern Appalachian Mountains and foothills (300–1000 m a.s.l.) North Carolina to Pennsylvania, in several forest types, such as Quercus and Pinus mixed forests and Tsuga canadensis-Betula alleghaniensis forests. Typically occurring in humid areas, such as streambanks or other mossy, wet areas; hypogeous or erumpent, often erumpent in moss-covered areas near streams or from sediment in steep streambanks, occurring singly or in scattered clusters. Collected late summer, fall and early winter (August–December). Presumed ectomycorrhizal based on fruiting habit and isotopic data.

Additional materials examined: USA, North Carolina, Henderson Co., Mills River, Pisgah National Forest, Pinus strobus woodlands with some Quercus, Rhododendron, and Oxydendrum arboreum, erumpent in mineral soil on creek banks, 680 m elev. 27 Dec. 2021, A. Muscat BL368 (FLAS-F-68880); ibid., B. Lemmond BL369 (FLAS-F-68881); ibid., B. Lemmond BL370 (FLAS-F-68882), ibid., 31 Jul. 2022, D. Upchurch BL525 (FLAS-F-71195); North Carolina, McDowell Co., Armstrong Creek, under Tsuga canadensis and Quercus in a riparian habitat, 12 Sep. 1998, O.K. Miller JT23199 OKM 27447 (OSC131663); North Carolina, Macon Co., Highlands Biological Station, Coker Rhododendron Trail, erumpent in shady streambank with Rhododendron, Betula allegheniensis, Tsuga canadensis, and Quercus spp. nearby, 1175 m. elev., 9 Sep. 2021, G. Bonito & B. Lemmond BL326 (FLAS-F-68722); ibid., Nantahala National Forest, Bull Pen Road, near Old Iron Bridge along Chattooga River, 735 m elev., erumpent in moss in riparian area, 5 Sep. 2021, L. Kaminsky (FLAS-F-68345); ibid., 7 Sep. 2021, L. Kaminsky (FLAS-F-68513); ibid., along Nantahala River Bike Trail, 600 m elev., erumpent in soil in riparian area, 8 Sep. 2021, G. Bonito (FLAS-F-68634); ibid., erumpent in soil and duff in a steep stream bank, 610 m elev., 8 Sep. 2021, R. Healy (FLAS-F-68644); North Carolina, Transylvania Co., Pisgah National Forest, Pink Beds Loop, 1000 m elev., 26 Aug. 2023, D. & J. Bower iNaturalist #180286100 BL587 (NAMA2023-456, FLAS-F-71876); Tennessee, Sevier Co., Great Smoky Mountains National Park, along bank of Injun Creek near Greenbrier Ranger Station, 17 Aug. 2021, B. Lemmond BL303 (FLAS-F-68248).

Notes: Description adapted from Lange (1950), Trappe & Sundberg (1977), and Kovács et al. (2008) with additional measurements and observations of fresh material. "Secondary wall" sensu Gibson & Kimbrough (1988) is used in place of "epispore" (Kovacs et al. 2008) to describe the amorphous and pitted outermost layer of the spore. The type material, preserved at the University of Copenhagen Herbarium (C), is immature, as discussed in Trappe & Sundberg (1977). However, an ITS sequence from the type specimen (GenBank EU327193) clearly falls within the *I. pachyascus* clade (Fig. 2). We do not designate a neotype here since the identity of the type specimen is clear, despite its lack of fully representative morphological features.

We examined two recent collections of I. gigantea from Japan (KPM-NC 23355, KPM-NC 29757) as well as a collection by Sanshi Imai from the type locality (Gilkey781, OSC146661) and found no consistent microscopic differences between I. gigantea and I. pachyascus, a conclusion shared by other authors who have examined both Japanese and North American specimens (Gilkey 1947, Trappe & Sundberg 1977, Kovács et al. 2008). Although Gilkey noted some differences in spore size between the single North American specimen she examined and the dimensions reported by Imai (1933), our examination of multiple specimens from North America and Japan revealed no consistent difference in spore dimensions. However, Imaia pachyascus specimens are notably smaller than I. gigantea, which can reach up to 15 cm in diameter, while the largest *I. pachyascus* specimens recorded thus far are 8 cm in diameter. Imaia pachyascus also has larger and more pyramidal warts, a thicker excipulum (up to 4 mm), and a deeper yellow brown peridium colour than I. gigantea or I. kuwohiensis (see below), which both have a pale whitish yellow peridium, thin excipulum (< 0.5 mm), and small, scaborous warts rather than large pyramidal warts. Mature specimens of I. pachyascus have a rich and pleasing aroma and flavour, while I. gigantea does not have a strong or pleasing aroma (I. kuwohiensis is only known from one collection, which had a strong disagreeable aroma – see below). The geographic separation and genetic differentiation in ITS and LSU (Fig. 2) and SSU (Kovács et al. 2008) between I. pachyascus and I. gigantea specimens further support the resurrection of *I. pachyascus* as a distinct taxon from eastern North America.

Imaia kuwohiensis Lemmond, M.E. Sm. & Noffsinger, *sp. nov.* MB 853893. Fig. 8.

Etymology: Referring to *Kuwohi*, the Cherokee name of the mountain in the Appalachian range of eastern North America where the holotype specimen was collected.

Ascomata subglobose, irregular and slightly lobed, 2–4.3 cm diam. Whitish to pale brown at first, then darkening to yellow brown, surface textured with small brown scabers and larger brown warts, sometimes with red-brown colouration. Warts or scabers irregular in size, 0.2–1 mm wide. Aroma pungent, fishy, disagreeable. Excipulum tissue thin, yellowish, 165–500 µm (mean 300 µm) thick, composed of two layers. Ectal excipulum 65–175 µm (mean 122 \pm 48 µm) composed of large, subglobose to angular cells with thick walls, the outermost yellowish to yellow brown, especially at wart apices, but becoming hyaline towards interior. Cells



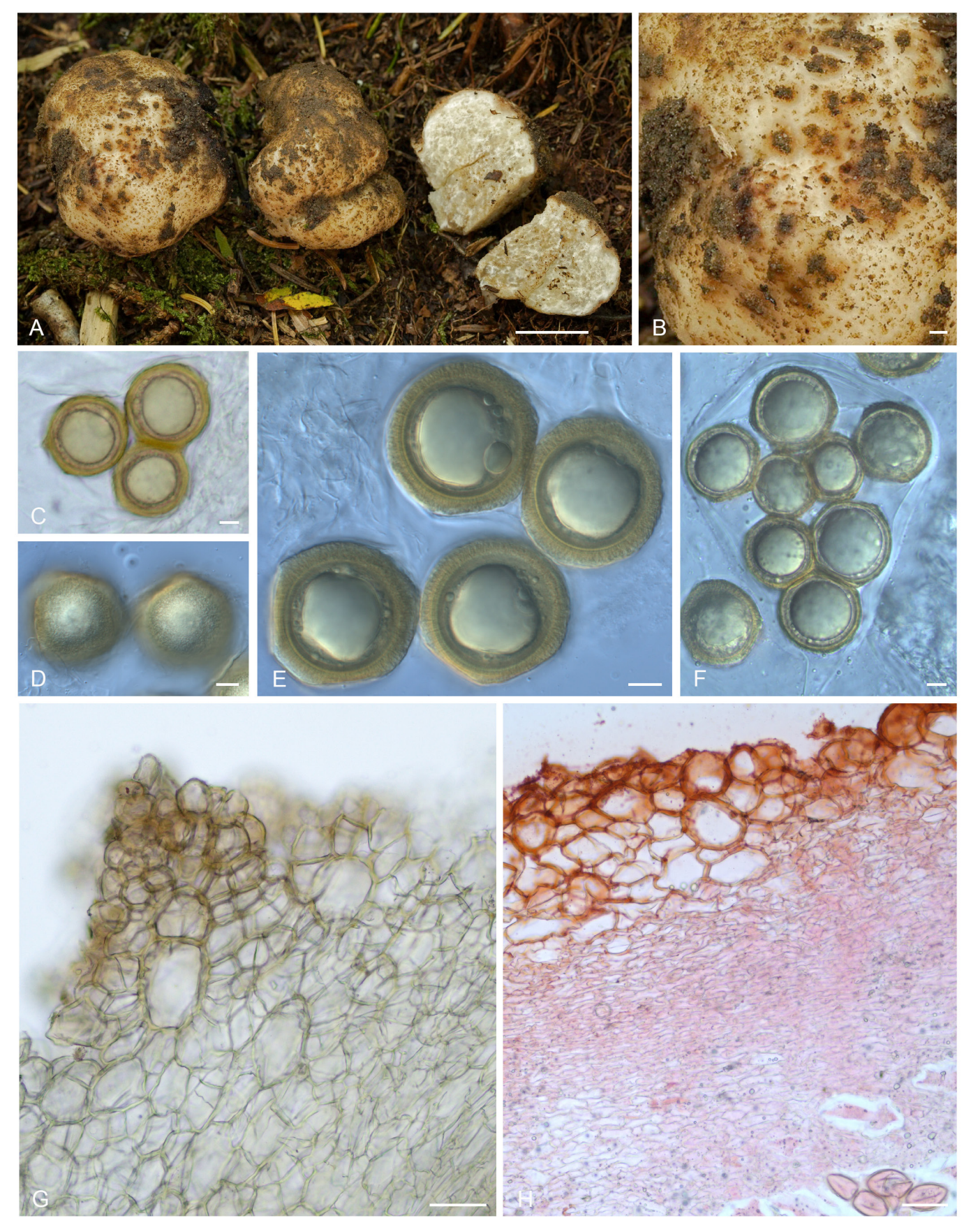


Fig. 8. Imaia kuwohiensis sp. nov. A. Fresh truffles. B. Closer view of scabrous and irregularly verrucose excipulum. C. Mature ascospores. D. Ascospores with mucilaginous secondary wall in focus. E. Ascospores. F. Ascospores in ascus. G. Cross-section through excipulum scaber. H. Cross-section of excipulum stained with Congo red, showing ectal and medullary excipulum layers and gleba with ascospores. Scale bars: A = 1 cm; B = 1 mm; $C-F = 10 \mu m$; $C-F = 10 \mu m$.

 $15-45 \mu m$ diameter (mean $31 \pm 13 \mu m$), walls $2.5-5 \mu m$ thick. Medullary excipulum 85–170 μ m thick (mean 168 ± 85 μ m), cells hyaline, compressed and appearing flattened or linearly arranged, cells 5-13 µm wide at septa. Gleba white, with sterile tissue mottled by grey brown fertile pockets, hyphae similar to medullary excipulum, 5-13 µm wide at septa, hyaline. Asci randomly arranged within fertile pockets in the gleba, ellipsoid, asci rarely with a pedicel, asci with 5-8 spores (mostly 8) per ascus; asci 127–171 (mean 149 ± 19) × 97-137 (mean 120 ± 18) µm, pedicel $17-28 \times 7-17$ µm (only n = 2 pedicels observed). Ascospores globose to subglobose or sub-polygonal, yellow brown at maturity with a thick wall and a single, large oil droplet inside, spore surface appearing finely pitted or ornamented due to mucilaginous secondary wall. Secondary wall sometimes flattened where spores are appressed to one another during development. Ascospores (including secondary wall) 33-51 (mean 42.2 \pm 4) \times 31-46 (mean 41.2 ± 3.5) μ m, Q = 1–1.13 (mean 1.05 ± 0.03).

Typus: **USA**, Tennessee, Sevier County, Kuwohi (formerly referred to as "Clingman's Dome"), Great Smoky Mountains National Park, along the Appalachian Trail near Fork Ridge trailhead, 1768 m a.s.l. with *Abies fraseri*, *Picea rubens*, and *Betula alleghaniensis*; next to roots of *A. fraseri*, 28 Sep. 2021, *C. Noffsinger*, CRN427 (holotype designated here TENN-F-077356, isotype FLAS-F-72460).

Distribution & Ecology: Known only from a mountaintop Abies fraseri-Picea rubens forest in the southern Appalachian Mountains along the Tennessee-North Carolina border at approximately 2000 m elevation. Hypogeous or erumpent in exposed soil banks, occurring as a cluster of several truffles. Presumed to be ectomycorrhizal with Pinaceae hosts.

Notes: This species can be distinguished morphologically from I. pachyascus and I. gigantea by its pale, light tan ground colour that is visible between darkened scabers, the scabrous peridium exterior which only occasionally forms larger subpyramidal warts, and the thin peridium layer. These features are similar to *I. gigantea*, which is only known from Japan. While I. gigantea is distinct for its large size and mild aroma and flavour, the variability of aroma and size are unclear for I. kuwohiensis, until further collections are made. However, phylogenetic analyses clearly support the separation of I. kuwohiensis and I. gigantea (Fig. 2) Other microscopic features of I. kuwohiensis such as spore and ascus characteristics, are virtually identical to *I. pachyascus* and I. gigantea. This species is only so far known from the spruce-fir habitat at approximately 2000 m elevation, from an area near the southernmost extent of this habitat type. Additionally, a high-throughput analysis of fungal soil sequences from spruce-fir habitats of the Southern Appalachians did not find any sequences identified to the family Morchellaceae, indicating that this species may be rare (Noffsinger & Matheny 2025). Phylogenetic and phylogenomic analyses clearly separate this species from the other North American Imaia species, I. pachyascus, which is known from a variety of habitats at lower elevations in the southern and mid-Atlantic Appalachian Mountains and foothills (Figs. 2-4). The epithet kuwohiensis, derived from the Cherokee place name Kuwohi, was used with approval from the Cherokee Speaker's Council (T. McCabe, pers. comm. April 2024).

Kalapuya M. Trappe, Trappe, & Bonito, *Mycologia* **102**: 1059. 2010.

Ascomata hypogeous, stereothecial, subglobose. Peridium purplish-brown or brown, warty, with warts separated by thin fissures. Gleba solid, whitish, with the fertile tissue grey brown and spotted. Asci ellipsoid or globose. Ascospores ellipsoid, smooth, hyaline (colourless) when young, ambercoloured at maturity.

Type species: Kalapuya brunnea M. Trappe, Trappe, & Bonito

Leucangium Quél., Compt. Rend. Assoc. Franç. Avancem. Sci. Assoc. Sci. France 11: 404. 1883. [1882].

Ascomata hypogeous, stereothecial, subglobose to slightly lobed. Peridium pink, purple, or black, composed of thick-walled isodiametric to angular cells that are sometimes raised in warts. Peridium often cracked and covered with fine hyphoid hairs that lack distinct bases. Gleba solid, white or pinkish, fertile tissue darker grey or grey-black and spotted. Asci globose, with (4–)6–8 ascospores. Ascospores fusiform, ends either apiculate or slightly rounded, light brown to olivaceous at maturity.

Typification: Leucangium carthusianum (Tul. & C. Tul.) Paol. (=L. ophthalomosporum Quél., Picoa ophthalmospora (Quél.) E. Fisch.)

Leucangium carthusianum (Tul. & C. Tul.) Paol., in Saccardo, *Syll. Fung.* (Abellini) **8**: 900. 1889.

Basionym: Picoa carthusiana Tul. & Tul., Fungi hypogei ed. alt.: 24. 1862.

Synonyms: Leucangium ophthalmosporum Quél., Compt. Rend. Assoc. Franç. Avancem. Sci. Assoc. Sci. France 11: 404. 1883 [1882]; Picoa ophthalmospora (Quél.) E. Fisch., Rabenhorst Kryptogamen-Flora. 1(5): 81. 1897.

Ascomata subglobose, 2-4 cm diam., firm, brown-violetblackish, surface rough to finely verrucose, occasionally erumpent from soil. Peridium not easily separated from the gleba. Aroma reported variously as melon-like (Quélet 1883, Fischer 1897), similar to Tuber mixtum (Tulasne & Tulasne 1862), similar to T. borchii (Paolocci 1889), or strong and unpleasant (Van Vooren 2017). Peridium of two intergrading layers: an ectal excipulum of textura globosa-angularis cells 15-60 µm diam., outermost cells purple black, projecting in many places beyond the excipulum surface in septate hair-like cells; medullary excipulum cells hyaline or pinkish, textura intricata. Gleba of hyaline textura intricata. Asci subglobose or broadly clavate, some with pedicels, randomly arranged within fertile pockets in the gleba, subglobose to ellipsoid, $90-150 \times 75-90 \mu m$, with (4-)6-8 spores per ascus (typically 8-spored). Ascospores citriniform to fusiform, pale golden-yellow to yellow brown with maturity, with one large or several smaller oil droplets, ascospores 42-78.2(-86) (mean 60.8 ± 7.44) × 17.6–35.2 (mean 27.5 ± 3.25), Q = 1.45–3 (mean 2.23 ± 0.32).

Typus: **France**, Auvergne-Rhône-Alpes, Isère, Saint-Pierrede-Chartreuse, near the Monastère de la Grande Chartreuse, Sep. 1857, det. *Tulasne & C. Tulasne*.

Additional materials examined: France, Bourgogne-Franche-Comté, Jura, Oct. 1899, leg. Hètier, det. (as L. ophthalmosporum) N.T. Patouillard (HUH: Patouillard 4525); Auvergne-Rhône-Alpes, Cantal, Cheylade, under Pinus sylvestris, 975 m a.s.l, several specimens shallowly erumpent from the ground, 25 Sep. 2014, leg. A.M. Andraud, det. N. Van Vooren NV 2014.09.39 (FLAS-F-68912). Greece, Peloponnese, Arcadia, Gortynia, Vytina, with Abies cephalonica, 1300 m a.s.l., 2021, leg. N. Oppicelli, det. A. Vizzini (FLAS-F-71147), ibid., Mainalo mountain, with A. cephalonica, 25 Nov. 2016, leg. M. Gkilas, det. V. Kaounas VK-4683 (FLAS-F-71990). Italy, Cuneo, Certosa di Pesio, Pian delle Gorre, under Abies alba and Pinus spp., 4 Mar. 2018, A. Vizzini (FLAS-F-71146). Poland, Lesser Poland, Tatra National Park, Wielka Sucha Dolina Valley, in coniferous forest (Abies, Picea), on calcareous bedrock, 970 m a.s.l., 24 Sep. 2019, M. Kozak & F. Karpowicz (KRA F-TPN/19/0357, FLAS-F-71993); ibid., N. slope of Hruby Regiel, above road from Zakopane, in coniferous forest (Abies, Picea), under Abies, 980 m a.s.l., 15 Oct. 2019, M. Kozak & J. Brańka (KRA F-TPN/19/0471, FLAS-F-71994); Lesser Poland, Gorce Mts., mouth of Za Palacem stream, in garden near buildings, close to the forest edge (Abies, Picea, Fagus), 650 m. a.s.l., 9 Nov. 2015, leg. E. Zając, det. P. Mleczko (KRA F-2015-3, FLAS-F-71995); Forędówki stream valley, in mixed forest (Abies, Picea, Fagus), on steep slope by a small stream, 860 m a.s.l., 10 Nov. 2012, leg. & det. M. Kozak & K. Kozłowska-Kozak (KRA F-2012-112, FLAS-F-71996).

Distribution & Ecology: Typically associated in upland habitats with various species of Abies, Picea, and Pinus; Tulasne & Tulasne (1862) describe collections from mixed forests of Abies and Fagus. Infrequently collected, but reported from a wide geographic distribution in western, southern, and central Europe. Presumed ectomycorrhizal with Pinaceae hosts.

Notes: Description adapted from Tulasne & Tulasne (1862), Quélet (1883), Fischer (1897), Paoletti (1889), Van Vooren (2017), and measurements of recent collections listed above. Multilocus and genome sequences of modern specimens matching the morphological description of *L. carthusianum* formed a strongly supported monophyletic clade in all analyses (Figs 2–4), and were morphologically and phylogenetically distinct from the other species present in Europe, *L. purpureum*. Because we were not able to examine the type specimens of either *L. carthusianum* or the presumed synonym *L. ophthalmosporum*, we have opted not to name an epitype for *L. carthusianum*. Future studies should examine the type specimens of *L. carthusianum* and *L. ophthalmosporum* to assess the validity of their synonymy and clarify their identities.

Leucangium cascadiense Lemmond & M.E. Sm., **sp. nov.** MB 853895. Fig. 9.

Etymology: Named for the Cascadia bioregion where this truffle occurs, which includes parts of British Columbia, California, Oregon, and Washington.

Ascomata subglobose to lobate, typically 3–5 cm diam. (up to 7 cm), lacking obvious basal attachment. Outer surface black or purple black, verrucose, warts variable across surface

but typically pyramidal, measuring 0.1-1.1 (mean 0.5) mm broad × 0.1–0.5 (mean = 0.25) mm tall. Aroma rich, fruity, and wine-like when fresh, with notes of chocolate especially distinct when dried. Excipulum 0.25-1.5 mm thick, composed of two layers: ectal excipulum (70-)150-580(-800) µm thick, composed of nearly isodiametric, inflated cells of textura globosa-angularis, cells 9-40 µm diam. (mean 25 ± 9.8 µm), outermost cells purple-brown, walls 1.5-2 µm thick, cell walls becoming less pigmented and thinner (1 µm thick) towards interior; medullary excipulum 120-690 µm thick (mean 295 µm) composed of hyaline, interwoven cells of textura intricata, cells mostly hyphal but some inflated, 5-33 µm (mean 10.7 ± 6 μm) at the septa, intergrading with glebal hyphae. A sparse tomentum is present in some areas of excipulum surface, especially in cracks and fissures in the peridium. Tomentum composed of septate, thick-walled purple-brown or pink hyphae projecting up to 225 µm from excipulum surface, cells 7-18 µm thick (mean 11.6 ± 3.8 µm) at septa and swollen in between, occasionally branching, intergrading with inflated cells of excipulum. Gleba composed of offwhite sterile hyphae mottled with irregular, blotchy patches of brown, greyish-brown, or brownish-black fertile tissue. Gleba hyphae of textura intricata which is also occasionally interspersed with inflated cells, cells 5-18(-27) µm wide at septa. Asci randomly arranged within fertile pockets in the gleba, subglobose, 95-150 (mean 116 \pm 12.7) \times 71-109 (mean 97.6 \pm 9.7) μ m, with 3–8 (mostly 8) spores per ascus. Ascospores typically citriniform with apiculate ends, goldenyellow, 45-99 (mean 69.6 \pm 9) × 22-37 (mean 29.9 \pm 2.5) μ m, Q = 1.3–3.5 (mean 2.3 \pm 0.4). Ascospore shape and dimensions highly variable, even within a single fruiting body; some ascospores lacking apiculate ends, appearing almost ellipsoid. Ascospores typically containing one large oil droplet.

Typus: **USA**, Oregon, Lincoln Co., Harlan, north side of Hilltop Rd. above Grant Creek, in 25-year-old *Pseudotsuga menziesii* timber stand, with scattered *Polystichum munitum* understory, ca 180 m a.s.l., 3 Apr. 2022, *J. Griffen* BL439 (**holotype** designated here FLAS-F-71176).

Additional materials examined: USA, Oregon, Benton Co., Starker Timber property off Hwy 20 midway between Blodgett, OR and Burnt Woods, OR, P. menziesii timber stand, 4 Apr. 2022, C. LeFevre BL441 (FLAS-F-71178); ibid., 8 Jan. 2005, G. Wilson & B. Myers JT30540 (OSC 111245); Oregon, Columbia Co., BLM Salem District, 27 Nov. 2001, S. Luce (OSC 117879); ibid., Warren, Nastrom's tree farm, 4 Feb. 2012, A. Beyerle JT36027/Beyerle 2478 (FLAS-F-72475); Oregon, Crook Co., Walton Lake, Ochoco National Forest, 23 Mar. 2022, Heather Dawson BL451 (FLAS-F-71097); Oregon, Lane Co., Lowell, Patterson Mountain Trail, 27 Mar. 2022, Heather Dawson BL450 (FLAS-F-71184); ibid., Greenleaf Creek Road, ca 0.5 km N of Hwy 36, 11 Mar. 2004, J. Getz JT29384 (OSC82191); Oregon, Lincoln Co., Along either side of Hilltop Rd above Grant Creek near Harlan, OR, P. menziesii timber stand, 3 Apr. 2022, H. & H. Dawson BL436 (FLAS-F-71173); ibid., BL438 (FLAS-F-71175); Oregon, Linn Co., Little Wiley Creek, 5 Jan. 1995, V. Moore JT17310 (OSC59163); ibid., Santiam Wagon Rd. near House Rock Campground, 12 Apr. 2006, R. Claremont JT31507 (OSC 112169); Oregon, Marion Co., about 7 mi. E. of Silverton, OR, young P. menziesii stand near agricultural fields, 2 Apr.

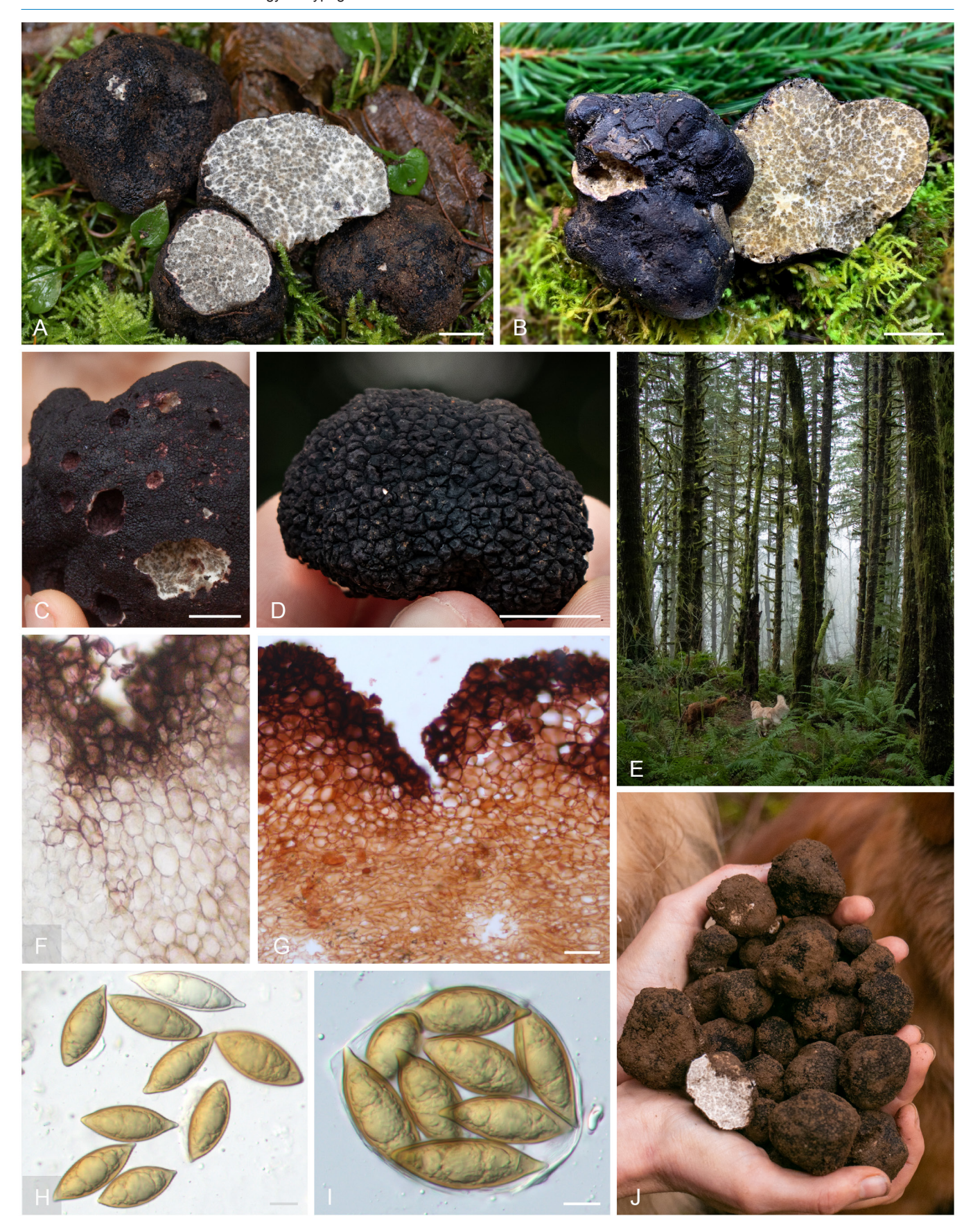


Fig. 9. Leucangium cascadiense sp. nov. **A, B.** Fresh truffles. **C, D.** Closer view of excipulum showing variation in colour and texture. **E.** Trained dogs finding *L. cascadiense* truffles in typical habitat dominated by *Pseudotsuga menziesii*. **F.** Cross-section of ectal excipulum with inflated purple-brown cells. **G.** Cross-section of excipulum stained in Congo red, ascus with ascospores. **H.** Loose ascospores. **I.** Ascus with ascospores. **J.** Fresh truffles harvested with the aid of trained dogs. Scale bars: A-D=1 cm; F, G=50 μ m; H, I=20 μ m.



2022, C. Lindstedt BL430 (FLAS-F-71167); ibid., BL432 (FLAS-F-71169); ibid., BL435 (FLAS-F-71172); Oregon, Multnomah Co., BLM Salem District, 19 Nov. 2001, S. Luce (OSC 117874); Oregon, Polk Co., Black Rock, Lackiamute Tree Farm, 5 Nov. 1994, Z. Carter JT13352 (OSC 59137); Washington, Clallam Co.,, DNR land near Sol Duc River W of Sappho, WA, mixed coniferous forest, 31 Mar. 2022, M. Donovan BL422 (FLAS-F-71161); ibid., Olympic National Forest, Soleduck Ranger District, 26 Nov. 2001, B. Annegers (OSC 117017); Washington, Cowlitz Co., Gifford Pinchot National Forest, Mt. St. Helens Ranger District, 18 Oct. 2000, S. Carin GIF-0454 (OSC 118565); Washington, King Co., near Stossel Creek, in P. menziesii timber stand with sword fern understory, ca 180 m a.s.l., 30 Mar. 2022, A. McGee BL419 (FLAS-F-71159); ibid., BL421 (FLAS-F-71160); Washington, Jefferson Co., N. of Dabob near Tarboo Creek, young (ca 20 yr) P. menziesii stand with sword fern understory, 1 Apr. 2022, A. McGee BL425 (FLAS-F-71162); ibid., BL426 (FLAS-F-71163); ibid., BL427 (FLAS-F-71164); ibid., Coyle Peninsula, along Coyle Rd., 1 Apr. 2022, A. McGee BL429 (FLAS-F-71166); Washington, Skagit Co., near Lake McMurray, in P. menziesii timber stand with sword fern understory, ca 300 m. a.s.l., 29 Mar. 2022, A. McGee BL408 (FLAS-F-71148); ibid., BL409 (FLAS-F-71149); ibid., BL410 (FLAS-F-71150); ibid., BL411 (FLAS-F-71151); ibid., BL413 (FLAS-F-71153); ibid., BL417 (FLAS-F-71157); ibid., BL418 (FLAS-F-71158); Washington, Thurston Co., Fort Lewis Military Reservation, 18 Jul. 1995, D. McKay JT17246 (OSC131607). Canada, British Columbia, White Rock, 18 Oct. 1970, C. Wrase JT3223 (OSC131603).

Distribution & Ecology: Ectomycorrhizal with Pseudotsuga menziesii (Douglas-fir) and possibly other Pinaceae hosts. Hypogeous, typically 5–15 cm underground, but occasionally up to 25 cm deep, usually occurring singly. Found in forests dominated by P. menziesii from British Columbia, Canada, to at least Marin County, California (see iNaturalist observation 179481697), but possibly further south. Most abundant in coastal forests but also occasionally observed at inland sites in the Cascade Mountains. Collections of L. cascadiense at lower elevations (< 1000 m) are most abundant in the fall and spring (October–April), but some collections of this species have been reported year-round, particularly in the Pacific Coast Range. At higher elevations (1000–1500 m) in the Cascade Mountains, abundance peaks in the May–June snowmelt season.

Notes: This species has long been considered a disjunct population of L. carthusianum originally described from France, due to the morphological similarity between L. cascadiense and L. carthusianum (Gilkey 1954b, Trappe 1971). Leucangium cascadiense fits many of the macroscopic characteristics of the description of L. carthusianum, such as the violet black peridium with sparse, short hairs and a peridium composed of polygonal cells (Tulasne & Tulasne 1851). The spore dimensions reported in Tulasne & Tulasne (1851) for L. carthusianum are $60-80 \times 25-30 \mu m$, which fits most values (i.e., mean ± 1 s.d.) observed for L. cascadiense spores. We examined several specimens from Europe that matched the general description of L. carthusianum and formed a monophyletic clade (Figs 2–4), including collections from Greece, France, Italy, and Poland. Of those with mature

spores, the spores were 41-78 (mean 60.8 \pm 7.4) \times 17-35 (mean 27.5 ± 3.2) µm, with a Q ratio of 1.5-3.0 (mean 2.2 ± 0.3), making the spores of these European specimens on average slightly shorter and narrower, with a less elongated maximum Q ratio. However, the variation observed in spore measurements for L. carthusianum and L. cascadiense specimens indicate spore dimensions cannot be used to discriminate between these two species. Leucangium carthusianum is reported to have warts that are not easily distinguished with the naked eye (Tulasne & Tulasne 1851), whereas the warts of L. cascadiense are prominent and easily visible. Leucangium carthusianum is also described as having a thin peridium, through which the underlying pale gleba colour is visible in some places (Tulasne & Tulasne 1851), whereas white patches are not visible through the peridium of L. cascadiense. Examination of additional fresh specimens from Europe may help clarify whether the peridium texture and colour is a consistent and a useful diagnostic feature to separate these two groups. Geographic separation and a clear genetic differentiation across all loci in the multilocus analysis and a majority of loci used in the phylogenomic analysis (Figs 3-4) support our conclusion that these two morphologically similar clades are distinct species. The large size (3-7 cm diam.) and purple-black excipulum of L. cascadiense clearly distinguish this species from the smaller, pink-coloured species L. purpureum, with which it co-occurs. The spores of L. cascadiense are (on average) longer (i.e. $45-99 \mu m$ long, mean $69.6 \pm 9 \mu m$) compared to L. microspermum (42.5-62 µm), but overlap with L. purpureum $(45-102 \mu m, mean 71.4 \pm 9.4 \mu m)$. The presence of prominent peridial warts further distinguishes L. cascadiense from two other species of Leucangium that have smooth peridia, L. microspermum and L. oneidaense (described below).

Leucangium cascadiense is an economically important edible truffle in many parts of the Pacific Northwestern USA and British Columbia, Canada, where it is often collected with the help of trained truffle dogs.

Leucangium oneidaense Lemmond, M.E. Sm. & DeSanto, sp. nov. MB 853896. Fig. 10.

Etymology: Named for Oneida County, New York, where the holotype specimen was found.

Ascomata subglobose, 4-8 cm diam., lacking obvious basal attachment. Outer surface black, smooth (not verrucose), cracked in many places with deep fissures exposing white excipulum tissue. Holotype specimen (PUL-F-26326) with irregular tomentum of pink-purple hyphae on excipulum surface, which is visible (with aid of a hand lens or dissecting microscope) as purplish hyphal tufts, especially prominent in cracks and fissures of the peridium; the other specimen (FLAS-F-73065) lacking any tomentum. Aroma subtle, grassy, or not distinctive. Excipulum 525-1065 (mean 739) µm thick, composed of two layers: ectal excipulum 155-690 (mean 387) µm, composed of purple-brown inflated, interwoven cells of textura globosa-angularis, cells 8-24 (mean 15) µm diam., some cells continuing from interwoven layer to project individually as septate, hair-like cells sometimes forming a scattered to dense tomentum. When present, tomentum hyphae septate, purple-brown, cells 8-24 µm (mean 14) wide at septa. Medullary excipulum 125-870 (mean 314)



Fig. 10. Leucangium oneidaense sp. nov. A. Fresh ascoma sliced to show gleba. B. Ascoma showing cracked exterior. C. Developing asci with pedicels. D. Ascospore. E. Fragment of dried excipulum tissue showing dense tomentum. F. Ascus with ascospores. G. Crack in excipulum showing pink-purple tomentum against white excipulum tissue. H. Ectal excipulum and tomentum. I. Interface of ectal and medullary excipulum layers. J. Gleba tissue (including ascus and ascospores) stained with Congo red. Scale bars: A, B = 1 cm; C, F, H–J = 20 μ m; D = 10 μ m; E, G = 1 mm.

μm, composed of hyaline hyphae of textura intricata, cells $6.5{\text -}10~\mu\text{m}$ wide at septa, grading into hyaline glebal hyphae of textura intricata, cells $4{\text -}10~\mu\text{m}$ wide at septa. *Gleba* whitish mottled with pale greyish yellow fertile pockets. *Asci* randomly arranged within fertile pockets in the gleba, subglobose to ellipsoid, narrowing abruptly to a tapered pedicel. Ascus portion containing spores $90{\text -}150$ (mean 123 ± 21) × $55{\text -}80$ (mean 72 ± 6) μm, pedicel (measured on detached asci) $25{\text -}38$ (mean 33 ± 6) μm long, tapering from $10{\text -}15~\mu\text{m}$ at the main part of the ascus to $4{\text -}6~\mu\text{m}$ the point where the pedicel meets the rest of the ascus. Asci with $2{\text -}8$ (mostly $6{\text -}8$) spores per ascus. Ascus walls thin (< $1~\mu\text{m}$). *Ascospores* citriniform, yellow brown, typically with one large oil droplet, spores $39{\text -}57$ (mean 47.3 ± 3.8) × $20{\text -}26$ (mean 24.3 ± 1.4) μm, $Q = 1.5{\text -}2.4$ (mean 1.9 ± 0.19).

Typus: **USA**, New York, Oneida Co., Camden, Costello Ave., erumpent in soil near *Tsuga canadensis* and *Betula* sp. on a steep bank down to a paved path, about 6 m from a river, ca 140 m a.s.l., 23 Oct. 2019, *P. DeSanto* 04402 (**holotype** designated here PUL-F-26326, **isotype** FLAS-F-72461).

Additional material examined: **USA**, Massachusetts, Berkshire Co., Beartown State Forest, mixed hardwood forest occurring near *Carya* sp., 5 Oct. 2024, leg. *E. Noble*, det. *A. Sow* (FLAS-F-73065).

Distribution & Ecology: This species is thus far only known from two collections from northeastern USA. The holotype collection was erumpent from soil and Tsuga canadensis duff in a forest with T. canadensis and other mixed hardwoods, while the other collection from Massachusetts was found near a Carya sp. tree in a forest of mixed hardwoods, suggesting the potential for a broader host range than other Leucangium species (i.e. with angiosperms and Pinaceae, instead of exclusively with Pinaceae). Additional specimens and observations are needed to determine more about the distribution and ecology of this species.

Notes: Leucangium oneidaense is clearly distinguished from other North American Leucangium species by several characteristics. The peridium of *L. oniedaense* lacks verrucae, and is sometimes densely tomentose in places, especially in cracks and fissures in the peridium, while excipular hairs are only sparsely present on L. cascadiense and L. purpureum. The purple black peridium colour clearly differentiates L. oneidaense from the pinkish to pale violet L. purpureum, and the lack of verrucae in L. oneidaense differentiates it from L. cascadiense. Microscopically, the spores of L. oneidaense are much smaller than any other Leucangium species except for L. microspermum from Japan. Leucangium oneidaense closely resembles L. microspermum in several ways, including shallowly hypogeous to erumpent habit, overall size, peridium appearance, and spore dimensions. Phylogenetic analysis of rDNA sequences, however, clearly differentiates L. oneidaense from L. microspermum (Fig. 2), along with their geographic separation on different continents.

Leucangium oneidaense is thus far known only from two collections occurring in northeastern USA. These collections cluster together in all phylogenetic analyses and are morphologically consistent except for the lack of obvious hyphoid hairs making a tomentum in peridial fissures on the collection from Massachusetts. This may be a developmental difference, as the presence of hyphoid hairs is an inconsistent character in other species, and these hairs are most often observed (in any *Leucangium* species) in cracks and fissures in the peridium. These hairs are not distinct from ectal excipular cells except for their growth outwards beyond the peridium surface. Additional collections may help clarify the status of hyphoid hairs on the peridium as a distinguishing trait of this species, and its relation to developmental stage of individual ascomata.

Leucangium purpureum (L. Fan & M. Chen) Lemmond & M.E. Sm., comb. et stat. nov. MB 853897. Fig. 11. Basionym: Leucangium carthusianum var. purpureum L. Fan & M. Chen, Phytotaxa 347: 168. 2018.

Ascomata subglobose, lobate, typically 0.5-3 cm diam., lacking obvious basal attachment. Outer surface pinkish brown or rose pink with whitish patches, smooth to finely verrucose. Aroma fruity, wine-like. Excipulum 100-700 µm (mean 265 μm) thick composed of two distinct layers: ectal excipulum 20-420 µm (mean 142 µm) of inflated cells of textura intricataangularis, outermost cells pink-brown, cells 10-55 µm diam., walls up to 2.5 μm thick; medullary excipulum 10-370 μm (mean 140 µm) thick composed of hyaline hyphae of textura intricata, cells 4-10 µm wide at septa. A sparse tomentum is occasionally present in some areas of the excipulum surface, especially in cracks and fissures in the peridium, projecting up to 270 µm from excipulum surface, cells 7-16 µm wide at septa. Gleba whitish mottled with greyish, blotchy patches of fertile tissue. Gleba hyphae hyaline, textura intricata, 4-10 µm wide at septa. Asci randomly arranged within fertile pockets in the gleba, ellipsoid, (95–)115–172 (mean 135 \pm 18) × (55–)62-88(-100) (mean 76 ± 9.4) μ m, with 3-8 (mostly 8) spores per ascus. Ascospores citriniform to fusiform to elongatefusiform, 45-102 (mean 71.4 \pm 9.4) \times 15-31 (mean 23.8 \pm 3.1) μ m, Q = 1.8–5.5 (mean 3.0 ± 0.6).

Typus: **China**, Hebei, Wuling Mountains, in the soil under *Larix principis-rupprechtii*, 13 Aug. 2015, *Hanling 002* FAN496 (**holotype** BJTC).

Additional materials examined: Canada, British Columbia, Maple Ridge, 15 Jul. 1992, H. Massicotte & L. Tackaberry JT12798 (OSC 131592). Poland, Lesser Poland, Sucha County, Skawica, Beskid Żywiecki Mountains, Babia Góra Range, in the middle part of the Skawiczanka Stream Valley. in mixed forest (Abies, Fagus, Picea), 550 m a.s.l., 28 Jun. 2012, M. Kozak (KRA F-2012-38; FLAS-F-71992); Lower Silesian, Kłodzko County, Kletno, Mt. Śnieżnik, in mixed forest (Picea, Fagus), 710 m a.s.l., 20 Jul. 2013, M. Kozak & K. Kozłowska-Kozak (KRA F-2013-35, FLAS-F-71991). USA, New Hampshire, Coos Co., Dartmouth College Second College Grant, mixed hardwood forest, composite sample of rodent scat from multiple rodent species captured in traps over a two-month period, Jul./Aug. 2018, R. Stephens BL577 (FLAS-F-71903); ibid., spore sample from Tamias striatus scat filtered and suspended in ETOH (FLAS-F-72474); Oregon, Coast Range, under Pseudotsuga menziesii, 1 Jun. 1995, J. Bolton JT17224 (OSC 131636); Oregon, Clackamas Co., Mount Hood National Forest, Still Creek campground, 31 Oct. 2007, J. Paque JT35404 (OSC 130939); Oregon,



Fig. 11. Leucangium purpureum comb. et stat. nov. **A.** Fresh truffles. **B.** Close-up of gleba. **C.** Cross-section showing ectal and medullary excipulum and gleba with ascospores. **D.** Ectal excipulum with inflated cells and thin outermost layer of brown-pink cells. **E.** L. purpureum from Poland. **F.** Gleba tissue stained with Congo red. **G.** Asci with ascospores (pink colour from residual Congo red). **H.** Elongate ascospores. **I–L.** L. purpureum spores from mycophagous mammal scat samples, FLAS-F-72474 (I, J) and FLAS-F-71903 (K, L) from eastern USA. Scale bars: A, C, E = 1 cm; B = 1 mm; C, D = 50 μm; F–L = 20 μm.

Jefferson Co., Jack Lake Trail, with Tsuga mertensiana and Abies sp., 7 Oct. 2023, H. Dawson FUNDIS 52398, iNaturalist #188112392 (FLAS-F-72469); Oregon, Jefferson Co., Sisters, Jack Lake Trail, with Abies and Pinus, 8 Oct. 2022, H. Dawson FUNDIS 52398 (FLAS-F-71197); Oregon, Klamath Co., Vivian Lake Trail, Deschutes National Forest, Hwy 58 (43.594538, -122.142403), T. mertensiana, Abies sp., P. menziesii overstory, 25 Nov. 2022, H. Dawson BL576 (FLAS-F-71869); Oregon, Lane Co., Blachly, Greenleaf Creek Rd., P. menziesii forest with Polystichum munitum understory, 12 Jun. 2022, H. Dawson BL518 (FLAS-F-71191); Oregon, Lane Co., Under P. menziesii, 12 May 2014, J. Frank JLF-3803 (FLAS-F-72470); Oregon, Lincoln Co., Yachats, Cook's Ridge Trail, P. menziesii forest with Polystichum munitum fern understory, 10 Sep. 2022, H. Dawson BL519 (FLAS-F-71192); Oregon, Marion Co., Scotts Mill, near Echo Creek Falls, 25 year afforested P. menziesii forest with Polystichum munitum understory, shallowly hypogeous, 2 Jun. 2020, C. Lindstedt BL386 (FLAS-F-68919); Oregon, Polk Co., W. of Falls City, Luckiamute Tree Farm, (44.87888889, -123.6491667), with P. menziesii, 3 Jun. 1995, M. Harvey JT17201 (FLAS-F-72471); Oregon, Polk Co., Peedee, Bald Mountain Rd., 1-2 miles from Peedee Creek Rd., with P. menziesii, 3 Jun. 1998, W. Bushnell JT22831 (FLAS-F-72472); Oregon, Tilamook Co., Ben Smith block, moderate thinning, station A6, T1N R7W sections 14-15, with P. menziesii, 16 Jun. 1996, M. Mahrt JT22763 (FLAS-F-72478); ibid., Cedar Creek, Deer-Diamond block control T2N R7W west half of section 31, with P. menziesii, 24 Jun. 1997, E. van Hollenbeck JT22764 (FLAS-F-72473); ibid., Siuslaw National Forest, Cascade Head Experimental Forest, summit, with P. menziesii and Tsuga heterophylla, 13 Oct. 1970, J. Trappe JT2303 (OSC 131590); ibid., with P. menziesii, J. Trappe JT2332 (OSC 131591); Oregon, Wasco Co., Bear Springs, with P. menziesii, 26 Sep. 1964, C. Goetz JT13027 (OSC 131618); Washington, King Co., Carnation, with P. menziesii, 30 Jun. 2019, D. Upchurch DU-16 (NCU-F-0031569); Washington, Snohomish Co., Monroe, with P. menziesii, 30 Jun. 2019, D. Upchurch DU-17 (NCU-F-0031570).

Distribution and Ecology: This species is found on multiple continents in the northern hemisphere and is associated with Pinaceae hosts. Ascoma have been collected from China, western USA and Canada, and Poland. The holotype collection, from the Wuling Mountains in central China, was collected under Larix principis-rupprechtii. In North America, L. purpureum is most often found in the Cascadia bioregion that includes the coastal forests and Cascade Mountains (up to ca 1500 m a.s.l.) from British Columbia, Canada to Oregon, USA, typically in association with Pseudotsuga menziesii (Douglas-fir) and other Pinaceae trees (e.g. Tsuga mertensiana, Abies sp.). Two spore samples isolated from mammal scat were collected in eastern North America from mammals in a hardwood-dominated forest with some Pinaceae species present (Stephens et al. 2021, Borgmann-Winter et al. 2023). Leucangium purpureum is presumed ectomycorrhizal based on habitat, isotopic evidence, and known ECM trophic mode of the related species L. cascadiense.

Notes: Leucangium purpureum is a widespread species that occurs on multiple continents associated primarily with

Pinaceae hosts. All ascoma collections of this species share certain morphological similarities, particularly the pinkish hue of the peridium, lack of prominent verrucae, and small size (1–3 cm diam.) relative to other *Leucangium* species (typically 3-7 cm diam.). We detected no significant morphological differences across samples from different continents. Collections of L. purpureum in the Pacific Northwestern USA and southwestern Canada have been referred to in GenBank sequence accessions as "L. carthusianum var. amaretto" or informally by collectors as the "pink Leucangium" (J. Trappe, pers. comm.). Leucangium purpureum is easily distinguished macroscopically from L. carthusianum, L. cascadiense, L. microspermum, and L. oneidaense by its rosy pink peridium, smaller size and typical occurrence in groups or clusters. Microscopically, L. purpureum differs from L. carthusianum, L. cascadiense, L. microspermum, and L. oneidaense by its thinner peridium, lightly pigmented (brownish pink rather than purple black) ectal excipulum cells, and spores that are longer and narrower than L. microspermum or L. oneidaense and typically higher in length-to-width (Q) ratio than L. carthusianum and L. cascadiense (up to 5.5 in L. purpureum). However, spore characteristics of L. carthusianum, L. cascadiense, and L. purpureum are overlapping and can be highly variable, even within individual sporocarps.

DISCUSSION

Here we present the first modern, comprehensive study of the hypogeous Morchellaceae. In this work we performed the first phylogenomic analysis of this group to provide a robust view of the evolutionary relationships in these fungi (Fig. 4). Our data show that the hypogeous taxa in Morchellaceae (members of the four genera Fischerula, Imaia, Kalapuya, and Leucangium; Table 1) belong to a well-supported clade that is clearly differentiated from epigeous Morchellaceae and outgroup taxa. All of our multigene analyses (1497 BUSCO loci, 52 UFCG core genes, LSU+tef1+rpb2) support a single clade of truffle-forming genera that is sister to the epigeous, apothecial Morchellaceae genera (Figs 3-4). There is some conflicting signal at deeper nodes of the phylogenomic tree, which suggests uncertainty in the topology of some branches of the tree. For example, the phylogenomic trees suggest that Imaia and Leucangium are sister groups whereas Imaia and Kalapuya were sister groups in the three-locus phylogenetic analysis (Figs 3-4). We also found significant conflicting signal in the branches at the transition between epigeous Morchellaceae and the truffle taxa, particularly in the placement of the epigeous taxa in Verpa and Disciotis

The well-supported clade of truffle-like *Morchellaceae* fungi have long been presumed to interact with trees via the ectomycorrhizal symbiosis (e.g. Trappe 2009, Lefevre 2013). However, previous evidence was relatively scant with only a few individual root tip sequences (that lacked morphological data), poorly substantiated morphological analyses of ECM roots (lacking verification with molecular data) or isotopic signatures indicative of biotrophic lifestyles (but without direct evidence of ECM formation). In this study we used truffle-detecting dogs to locate truffles and collect fresh, healthy ECM root tips of *Pseudotsuga* colonized by *Leucangium cascadiense* from five different sites in Oregon

Table 1. Accepted genera and species of hypogeous *Morchellaceae*.

Genus	Species	Known Distribution	Synonyms	Reference
Fischerula	F. macrospora (TYPE)	Europe	_	Mattirolo (1928)
	F. subcaulis	Western North America	_	Trappe (1975)
Imaia	I. gigantea (TYPE)	Asia (Japan)	Terfezia gigantea Imai	Kovács et al. (2008)
	I. pachyascus	Eastern North America	Picoa pacyhascus Lange	This paper
	I. kuwohiensis	Eastern North America	_	This paper
Kalapuya	K. brunnea (TYPE)	Western North America	_	Trappe et al. (2010)
Leucangium	L. carthusianum (TYPE)	Europe	Picoa carthusiana Tul & C. Tul.	_
			Picoa ophthalmospora (Quél.) Fisch.	_
			L. ophthalmosporum Quél.	_
	L. cascadiense	Western North America	_	This paper
	L. purpureum	Asia (TYPE), Europe, and North America	Leucangium carthusianum var. purpureum L. Fan & M. Chen	Chen & Fan (2018)
	L. microspermum	Asia	_	Yamamoto et al. (2020)
	L. oneidaense	Eastern North America	_	This paper

and Washington, USA. These ECM roots had a consistent morphology of smooth, dark-brown mantle with no emanating cystidia (Fig. 5) and produced ITS sequences that clustered in a supported monophyletic clade with *Leucangium* truffles collected at the same sites (Fig. 2). Our morphological analyses of these ECM root tips showed intact plant root cells and a well-developed Hartig net, hallmark features of an ECM association (Fig. 5). Our findings firmly establish the ECM association between *L. cascadiense* and *P. menziesii* based on multiple lines of evidence including molecular, morphological, and isotopic analyses.

Although we were able to clearly establish the ECM symbiosis within the genus Leucangium, we unfortunately did not locate ECM root tips from members of the other focal genera (although DNA sequences from ECM roots were nested within the genus Fischerula in our ITS analysis - Fig. 2). The fact that we did not locate ECM roots from the other genera besides Leucangium may be due to the relatively low number of sites sampled, reflecting the rarity of some of these fungi compared to the relatively common *L*. cascadiense. To explore the trophic modes of the other taxa across Morchellaceae, we instead relied on C and N isotopic data from freshly collected fruiting bodies and fungarium specimens. Notably, all 18 specimens of Leucangium that were included in our analysis were resolved among other known ECM taxa and were predicted by the QDA model as ECM (Fig. 6, Table S3). Other hypogeous Morchellaceae that have previously been suspected to form ECM (including all tested samples from the genera Fischerula, Imaia, and Kalapuya) were also predicted by the model as ECM. This isotopic evidence further supports our hypothesis that the truffle-forming Morchellaceae rely on the ECM symbiosis with plants as their main source of carbon.

Interestingly, the trophic associations of some other genera within *Morchellaceae* were much less clear and deserve further study. We noted that members of the genera *Disciotis*, *Morchella*, and *Verpa* displayed a wide array of δ^{13} C/ δ^{15} N values, depending on the species and the sample. Samples from *Verpa* were predicted by the QDA model

as undetermined or saprotrophic, samples from Disciotis were precited as undetermined or ECM, and samples from Morchella were predicted as ECM, undetermined or saprotrophic (Fig. 6, Table S3). This wide range of values within epigeous *Morchellaceae* is interesting but is perhaps not surprising given the ongoing discussions in the literature about the trophic mode(s) of the genus Morchella (Dahlstrom et al. 2000, Hobbie et al. 2016, Loizides 2017, Healy et al. 2022). Some Morchella species can be cultured and grow readily as saprotrophs (Masaphy 2010, Ower 1982), but there is also evidence that at least some species can exist as endophytes in aerial plant tissues and also colonize roots (Baynes et al. 2012, Baroni et al. 2018). It is possible that these fungi may employ a mixed saprotrophic-biotrophic strategy or may switch between trophic approaches at different times of their lifecycle. Alternatively, it may be that species of Morchella have various trophic strategies and corresponding ecologies. Whatever the case, more detailed lab studies and comparative genomic approaches will be needed to further elucidate the trophic strategies in Morchellaceae, particularly the epigeous taxa. Future studies should further test our hypothesis that the truffle-like Morchellaceae form ECM whereas the epigeous Morchellaceae are non-ECM, despite having potential biotrophic phases or aspects to their lifestyles. It is interesting to note that the truffle-like morphology and the ECM trophic mode are often associated traits among other ECM fungi, particularly within Pezizomycetes (e.g. Læssøe & Hansen 2007, Tedersoo & Smith 2013). More work is needed to understand this phenomenon.

The transition to a truffle-like morphology prevents active (i.e. airborne) spore release, and truffles are therefore hypothesized to depend on animals as their main dispersal agents. In the case of the hypogeous *Morchellaceae* collected for this study, we found that they typically emitted strong odors at maturity and that trained dogs were able to readily locate them beneath soil or leaf litter that was sometimes up to 25 cm deep (Lemmond *et al.*, pers. obs.). Published studies from both eastern and western North America (Vernes *et al.* 2004, Gomez *et al.* 2005, Cloutier



et al. 2019, Sultaire et al. 2023) as well as from Europe (Komur et al. 2021) have documented Leucangium spores from mammal scat samples, thereby providing direct evidence of mammal dispersal of Leucangium spores. For example, a recent study by Sultaire et al. (2023) found evidence that the spores of both Leucangium cascadiense and L. purpureum (as Leucangium sp.) were dispersed by Townsend's chipmunks (Neotamias townsendii). We also provide additional evidence of Leucangium spore dispersal by mammals; samples FLAS-F-71309 and FLAS-F-72474 of mammal scats from New Hampshire, USA had spores of L. purpureum, which we included in our phylogenies with the help of Leucangium-specific PCR primers (Figs 2, 3). ITS sequences of L. purpureum were also generated in a previous study from eastern Canada (Cloutier et al. 2019). These samples constitute the only evidence of Leucangium present in eastern North America besides our newly described species, L. oneidaense. Additionally, Trappe (1975) reported a collection of F. subcaulis spores and tissue from stomach contents of the creeping vole, Microtus oregoni, collected in Oregon, noting that F. subcaulis represented about 95 % of the total stomach contents. Thus far, we know of no studies that have shown dispersal of Imaia or Kalapuya spores by mycophagous animals. This is not unexpected given that many of these taxa are relatively uncommon or have limited geographic distributions.

Our taxonomic additions and revisions to the hypogeous Morchellaceae significantly expand the known diversity of these fungi, and increase the geographic structure observed among these species. Collections of Imaia and Leucangium from separate continents (Asia, Europe, and North America) that were previously considered conspecific are now recognized as unique species with a more restricted geographic range. This is similar to the situation in other truffle-forming fungal clades, including within the Tuberaceae, where most species and even some larger phylogenetic clades are restricted to a single continent (Bonito et al. 2013). However, *L. purpureum* is a notable exception to this pattern, and we found evidence that this species occurs in Asia, western and eastern North America, and in central Europe (southern Poland). We found some support for phylogenomic separation of L. purpureum collections from North America and Europe (Fig. 4), though our multilocus analysis based on LSU, tef1, and rpb2 did not support continent-restricted clades. Since the type material of L. purpureum (or similar material from Asia) was not available for further study or sequencing and we detected no significant morphological differences across samples from different continents, we feel that a conservative approach requires that these continental groups not be separated into distinct species. Further study of the L. purpureum type material, as well as ascomata from other locations such as eastern North America (thus far only represented by mycophagous mammal scat samples), may reveal more extensive and consistent geographic structure among L. purpureum specimens.

Environmental sampling indicates that additional Fischerula and Leucangium species diversity also exists across the Northern Hemisphere. Based on our ITS phylogenies incorporating environmental data, there are at least two additional Fischerula species in North America and several undescribed Leucangium from Asia that are only known from environmental (soil, ECM) or mitotic spore

mat samples. For these species, fruiting bodies have yet to be discovered, which suggests that there will be future taxonomic work needed in these groups. Furthermore, we expect that concerted search for mitotic spore mats in areas where fruiting bodies of *Morchellaceae* truffles have been collected will help to reveal this life stage for other species of *Morchellaceae* truffles. To date, there is only one collection of a *Fischerula* anamorph from Minnesota, USA (Fig. 1C–E). Similarly, a mitotic spore mat of *Verpa* confirmed with DNA sequencing is reported here for the first time, from a collection in Kentucky, USA (FLAS-F-69662; see Table S1). Mitotic spore mats are evidently a consistent feature of the life cycle in several species of *Disciotis* and *Morchella* (Carris *et al.* 2015, Pfister *et al.* 2022).

Although several of the species included in our analysis have been rarely collected, the true rarity of these fungi and their sensitivity to particular habitats and environmental conditions is not well understood. Indeed, some of these fungi, particularly I. kuwohiensis, may be restricted to specific habitats such as the spruce-fir ridgetop forest ecosystems in the southern Appalachians. Abies fraseri (Fraser fir) is the only fir species found in the southern Appalachians and is endemic to this region (Smith & Nicholas 2000), where it occurs above 1500 m in elevation (Kaylor et al. 2017). Spruce-fir habitats of the southern Appalachians are threatened by numerous ongoing environmental issues such as atmospheric deposition, climate change, logging, and the invasive balsam woolly adelgid (White 1984, White & Cogbill 1992, Kaylor et al. 2017). Additionally, due to the ongoing effects of climate change, high-elevation habitats and ecosystems are highly threatened and projected to shift upward in elevation (Dirnnböck et al. 2011, McCain et al. 2021). Spruce-fir habitats are already restricted to the highest elevations in the southern Appalachians and could be reduced in geographic range or even eliminated in the future. Across the globe, mountain ranges contain a disproportionate number of rare species (Enquist et al. 2019), and the spruce-fir ecosystem of the southern Appalachians is known to contain a variety of rare and endemic species (Ford et al. 2015, Vagel et al. 2024). In this case, it is crucial to evaluate the conservation status of I. kuwohiensis and other hypogeous fungi, especially those in threatened ecosystems. Fungi are still poorly represented in conservation assessments, compared to other taxonomic groups (Dahlberg & Mueller 2011, Allen & Lendemer 2015, Davoodian 2015, Heilmann-Clausen et al. 2015). For instance, approximately 820 fungal species have been assessed for conservation status as part of the IUCN Red List initiative as of 2024, representing just 0.5 % of described fungal species (IUCN 2024). This figure is far fewer than the number of species of flowering plants (approx. 71000 species assessed, or 17 % of described species), insects (12750 species, 1.2 %), reptiles (10300 species, 84 %), or birds (11195 species, 100 %) (IUCN 2024). There are several types of data that are required to make informed decisions about conservation status. Most fundamentally, appropriate and consistent taxonomic designations are essential to define the units of study. Ecological knowledge of trophic mode, habitat niche, and symbiotic associations between fungi and other organisms (such as ECM host plants) is also essential for defining and modelling the potential niche of a species. With such foundational taxonomic and ecological information,

additional data on the distribution, population size, and trends in population can aid in making evidence-based conservation assessments (Dahlberg & Mueller 2011).

Collecting and studying hypogeous fungi, however, is inherently challenging. As with many other macroscopic fungal structures, truffles are ephemeral and produced only under certain conditions. Even in an environment where certain species are known to occur, their distribution is patchy and unpredictable. Systematic sampling by excavating soil can yield highly useful information, since a well-designed random sampling method allows for statistical inferences not possible with non-random methods (Stephens et al. 2017). However, these methods are time-consuming and laborious and more likely to miss rare taxa. Sampling scat from mycophagous animals is another effective and efficient way to detect the presence of hypogeous fungi and learn about their interactions with animal dispersers (Schickmann et al. 2012, Cloutier et al. 2019, Stephens & Rowe 2020, Borgmann-Winter et al. 2023, Caiafa et al. 2021, Komur et al. 2021, Stephens et al. 2021, Sultaire et al. 2023). Although we demonstrate in this study that these methods can detect taxa that are otherwise unknown, the fact that they only yield spores or DNA sequences limits their utility for taxonomic purposes. The use of trained dogs to collect truffles has long been a standard method for commercial truffle harvest, since trained dogs can be highly effective at finding truffles, preferentially seek out mature specimens, and minimize disturbance to the habitat compared to other methods (e.g. raking or systematic excavation). More recently, trained dogs are being employed in scientific surveys of truffle biodiversity (e.g. Molia et al. 2020, Dawson & Dawson 2024, Sow et al. 2024). The increased use of trained dogs for biodiversity research is a highly efficient approach that will be essential to documenting the habitat and geographic range, population size, and other types of data that are important for truffle biodiversity and conservation studies. Assessing conservation status of these truffles is particularly important given the interest that some of these species have attracted as culinary truffles.

Several ECM truffle fungi, primarily gourmet species in the genus Tuber, have been cultivated in semi-controlled conditions where truffle spores or mycelium are used to inoculate root tips of host plants grown in sterilized soil prior to transplanting to an orchard setting (Reyna & Garcia-Barreda 2014, Leonardi et al. 2019). Thus far, attempts to inoculate ECM host plants with various Morchellaceae truffle species have not been successful. While we demonstrate that L. cascadiense forms ectomycorrhizas with P. menziesii in nature, there may be other factors required for the formation of ECM roots in a controlled setting. For instance, despite decades of effort, the most expensive gourmet truffle, T. magnatum, evaded all attempts at inoculation on host plants and cultivation until only recently (Bach et al. 2021, Bach & Murat 2022). Now that we have shown that *L. cascadiense* forms ectomycorrhizas on P. menziesii roots in nature, future research can explore the mechanisms that facilitate this relationship. Elucidating some of the yet unknown factors needed for forming ectomycorrhizas and incorporating those into controlled experiments could yield insights into the trophic ecology of other hypogeous Morchellaceae.

ACKNOWLEDGEMENTS

The authors wish to thank S. Berch, Hilary Dawson, P. DeSanto, J. Eberhart, J. Griffen, C. LeFevre, C. Lindstedt, A. McGee, A. Muscat, E. Noble, K. O'Donnell, C. Paez, N. Van Vooren, A. Vizzini, D. Upchurch and several Truffle Dog Company students (and dogs) for contributing specimens and facilitating collecting expeditions. We also thank curatorial and collections staff at the FLAS, HUH, KRA, KPM, NCU, OSC, and PUL fungaria for providing specimens used in this research. We thank Kevin Childs and the MSU RTSF Genomics Core for assistance with sequencing genomic DNA samples. We thank A. Guber, M. Oerther and the Great Lakes Bioenergy Research Center for their assistance with processing stable isotope samples at MSU, and J. Curtis and the staff at the Stable Isotope Mass Spec Lab for processing isotope samples at UF. We thank J. Rollins and J. Konkol for their assistance with root tip sectioning and fluorescence imaging. We thank the Cherokee Speakers Council and T. McCabe for their guidance and review on appropriate application of the Cherokee word Kuwohi. We thank M. Dunlavey for her assistance with many aspects of permitting, site selection, and collection trip coordination in the Nantahala National Forest. We thank the U.S. National Park Service for their assistance with permitting and collections within the Great Smoky Mountains National Park.

Funding for this project was provided by NSF grants DEB-1946445 (to MES, GB, and RH), DEB-2106130 (to MES), DEB-2030779 (to P.B. Matheny in support of CRN), and an NSF GRFP Fellowship (no. 2019277707, to BL); additional support for conducting and sharing this research was provided by research scholarships to BL from the Mycological Society of America (MSA), the North American Mycological Association (NAMA), and the North American Truffling Society (NATS); and to CRN from the Tennessee Herbarium Hesler Endowment Fund.

Collection of *Imaia kuwohiensis* from the Great Smoky Mountains National Park was conducted under Permit No. GRSM-2021-SCI-2496. Collections of *Imaia pachyascus* from the Great Smoky Mountains National Park were collected under Permit No. GRSM-2021-SCI-2516. Specimens from the Nantahala National Forest were collected with written permission from the US Forest Service. Specimens from Highlands-Cashiers Land Trust property were collected with written permission from the Highlands-Cashiers Land Trust.

DATA AVAILABILITY

Alignments used in all phylogenetic and phylogenomic analyses are available on the Open Science Framework page associated with this project (https://osf.io/u5wkb/). Genome assemblies and raw sequence data used in this project are deposited on NCBI Sequence Read Archive under the BioProject accession PRJNA1112361.

Declaration on conflict of interest The authors declare that there are no conflicts of interest.

REFERENCES

- Allen JL, Lendemer JC (2015). Fungal conservation in the USA. *Endangered Species Research* **28**(1): 33–42. https://doi.org/10.3354/esr00678
- Alvarado P, Moreno G, Manjón JL, et al. (2011). First molecular data on Delastria rosea, Fischerula macrospora and Hydnocystis piligera. Boletín de La Sociedad Micológica de Madrid 35: 31–37.
- Astashyn A, Tvedte ES, Sweeney D, et al. (2024). Rapid and sensitive detection of genome contamination at scale with FCS-GX. Genome Biology 25: 60. https://doi.org/10.1186/s13059-024-03198-7
- Bach C, Beacco P, Cammaletti P, et al. (2021). First production of Italian white truffle (*Tuber magnatum* Pico) ascocarps in an orchard outside its natural range distribution in France. *Mycorrhiza* **31**(3): 383–388.
- Bach C, Murat C (2022). La production de la truffière à *Tuber* magnatum de Nouvelle-Aquitaine a augmenté en 2021! Le Trufficulteur 119: 17–18
- Baroni TJ, Beug MW, Cantrell SA, *et al.* (2018). Four new species of *Morchella* from the Americas. *Mycologia* **110**(6): 1205–1221. https://doi.org/10.1080/00275514.2018.1533772
- Baynes M, Newcombe G, Dixon L, et al. (2012). A novel plant-fungal mutualism associated with fire. Fungal Biology 116(1): 133–144. https://doi.org/10.1016/j.funbio.2011.10.008
- Benitez F (2021). How the Oregon truffle bends humans to its will.

 Oregon Public Broadcasting, May 18, 2021. https://www.opb.org/article/2021/05/18/superabundant-oregon-truffle-food-culture/ Accessed on March 26 2025.
- Benucci GMN, Lefevre C, Bonito G (2016). Characterizing rootassociated fungal communities and soils of Douglas-fir (*Pseudotsuga menziesii*) stands that naturally produce Oregon white truffles (*Tuber oregonense* and *Tuber gibbosum*). *Mycorrhiza* **26**(5): 367–376. https://doi.org/10.1007/s00572-015-0677-9
- Birkebak JM, Mayor JR, Ryberg MK, *et al.* (2013). A systematic, morphological and ecological overview of the *Clavariaceae* (*Agaricales*). *Mycologia* **105**(4): 896–911. https://doi.org/10.3852/12-070
- Bonito G, Smith ME, Nowak M, *et al.* (2013). Historical biogeography and diversification of truffles in the *Tuberaceae* and their newly identified Southern Hemisphere sister lineage. *PLoS ONE* **8**(1): e52765. https://doi.org/10.1371/journal.pone.0052765
- Borgmann-Winter BW, Stephens RB, Anthony MA, *et al.* (2023). Wind and small mammals are complementary fungal dispersers. *Ecology* **104**(6): e4039. https://doi.org/10.1002/ecy.4039
- Buscot F (1994). Ectomycorrhizal types and endobacteria associated with ectomycorrhizas of *Morchella elata* (Fr.) Boudier with *Picea abies* (L) Karst. *Mycorrhiza* **4**:223–232. https://doi.org/10.1007/BF00206784
- Bushnell, B (2014.). BBTools: a suite of fast, multithreaded bioinformatics tools designed for analysis of DNA and RNA sequence data. Joint Genome Institute. https://jgi.doe.gov/data-and-tools/software-tools/bbtools/ Accessed on 17 January 2024.
- Caiafa MV, Jusino MA, Wilkie AC, et al. (2021). Discovering the role of Patagonian birds in the dispersal of truffles and other mycorrhizal fungi. Current Biology 31(24): 5558-5570.e3. https:// doi.org/10.1016/j.cub.2021.10.024
- Capella-Gutiérrez S, Silla-Martínez JM, Gabaldón T (2009). trimAl: a tool for automated alignment trimming in large-scale phylogenetic analyses. *Bioinformatics* **25**(15):1972–1973.

- https://doi.org/10.1093/bioinformatics/btp348
- Carotenuto G, Genre A (2020). Fluorescent staining of arbuscular mycorrhizal structures using wheat germ agglutinin (WGA) and propidium iodide. In: *Arbuscular Mycorrhizal Fungi: Methods and Protocols* (Ferrol N, Lanfranco L., eds). Springer Nature, USA: 53–59.
- Carris LM, Peever TL, McCotter SW (2015). Mitospore stages of *Disciotis*, *Gyromitra* and *Morchella* in the inland Pacific Northwest USA. *Mycologia* **107**(4): 729–744. https://doi.org/10.3852/14-207
- Challis R, Richards E, Rajan J, et al. (2020). BlobToolKit Interactive quality assessment of genome assemblies. G3: GENES, GENOMES, GENETICS **10**(4):1361-1374. https://doi.org/10.1534/g3.119.400908
- Chen M, Fan L (2018). *Leucangium carthusianum* var. *purpureum*, a new purple truffle from China. *Phytotaxa* **347**(2): 165–175. https://doi.org/10.11646/phytotaxa.347.2.4
- Cloutier VB, Piché Y, Fortin JA, et al. (2019). A novel approach for tracing mycophagous small mammals and documenting their fungal diets. Botany 97(9): 475–485. https://doi.org/10.1139/cjb-2018-0222
- CNN (2022). This rare truffle has been the Appalachian Mountains' secret for over a decade. https://www.cnn.com/videos/travel/2022/07/04/Rare-Truffle-Appalachian-Mountains-Big-Trip-Orig.cnn Accessed on 26 March 2025.
- Czap, N (2012). In Oregon, truffles are no match for wet noses. The New York Times. August 12, 2012. https://www.nytimes.com/2012/08/08/dining/training-dogs-to-find-truffles-in-oregon.html Accessed on 26 March 2025.
- Dahlberg A, Mueller GM (2011). Applying IUCN red-listing criteria for assessing and reporting on the conservation status of fungal species. *Fungal Ecology* **4**(2): 147–162. https://doi.org/10.1016/j. funeco.2010.11.001
- Dahlstrom JL, Smith JE, Weber NS (2000). Mycorrhiza-like interaction by *Morchella* with species of the *Pinaceae* in pure culture synthesis. *Mycorrhiza* **9**(5): 279–285. https://doi.org/10.1007/PL00009992
- Danecek P, Bonfield JK, Liddle J, et al. (2021). Twelve years of SAMtools and BCFtools. *GigaScience* **10**(2):giab008. https://doi.org/10.1093/gigascience/giab008
- Davoodian, N (2015). Fungal conservation in the United States: current status of federal frameworks. *Biodiversity and Conservation* 24(8): 2099–2104. https://doi.org/10.1007/s10531-015-0935-3
- Darriba D, Taboada GL, Doallo R, *et al.* (2012). jModelTest 2: more models, new heuristics and parallel computing. *Nature Methods* **9**(8): 772. https://doi.org/10.1038/nmeth.2109
- Dawson HR, Dawson HA (2024). Use of a truffle dog provides insight into the ecology and abundant occurrence of *Genea* (*Pyronemataceae*) in Western Oregon, USA. *Ecology and Evolution* **14**(11): e70590. https://doi.org/10.1002/ece3.70590
- Edgar RC (2004). MUSCLE: multiple sequence alignment with high accuracy and high throughput. *Nucleic Acids Research* **32**(5): 1792–1797. https://doi.org/10.1093/nar/gkh340
- Fabreti LG, Höhna S (2022). Convergence assessment for Bayesian phylogenetic analysis using MCMC simulation. *Methods in Ecology and Evolution* **13**(1): 77–90. https://doi.org/10.1111/2041-210X.13727
- Fischer E (1897). Tuberaceen und Hemiasceen, in Rabenhorst Kryptogamen-Flora 1(5):81.
- Fauchery L, Uroz S, Buée M, et al. (2018). Purification of fungal high molecular weight genomic DNA from environmental samples. In: Fungal Genomics. Methods in Molecular Biology (de Vries R,

- Tsang A, Grigoriev I, eds) **1775**. Humana Press, USA: 21–35. https://doi.org/10.1007/978-1-4939-7804-5_3
- Fry, B (2007). Coupled N, C and S stable isotope measurements using a dual-column gas chromatography system. *Rapid Communications in Mass Spectrometry* **21**:750–756. https://doi.org/10.1002/rcm.2892
- Gardes M, Bruns TD (1993). ITS primers with enhanced specificity for basidiomycetes application to the identification of mycorrhizae and rusts. *Molecular Ecology* **2**(2): 113–118. https://doi.org/10.1111/j.1365-294X.1993.tb00005.x
- Gibson JL, Kimbrough JW (1988). Ultrastructural observations on Helvellaceae (Pezizales). Ascosporogenesis of selected species of Helvella. Canadian Journal of Botany 66(4): 771–783. https://doi.org/10.1139/b88-114
- Gilkey HM (1947). New or otherwise noteworthy species of *Tuberales*. *Mycologia* **39**(4): 441–452. https://doi.org/10.2307/3755176
- Gilkey HM (1954a). Taxonomic notes on *Tuberales*. *Mycologia* **46**(6): 783–793. https://www.jstor.org/stable/4547889
- Gilkey HM (1954b). Tuberales. North American Flora 2: 1-29.
- Gomez DM, Anthony RG, Hayes JP (2005). Influence of thinning of Douglas-fir forests on population parameters and diet of northern flying squirrels. *Journal of Wildlife Management* **69**(4): 1670–1682. https://doi.org/10.2193/0022-541X(2005)69[1670:IOTOD F]2.0.CO;2
- Healy RA, Arnold AE, Bonito G, et al. (2022). Endophytism and endolichenism in *Pezizomycetes*: the exception or the rule? *New Phytologist* **233**(5): 1974–1983. https://doi.org/10.1111/nph.17886
- Healy RA, Smith ME, Bonito GM, et al. (2013). High diversity and widespread occurrence of mitotic spore mats in ectomycorrhizal *Pezizales. Molecular Ecology* **22**(6): 1717–1732. https://doi.org/10.1111/mec.12135
- Healy RA, Truong C, Castellano MA, et al. (2023). Re-examination of the Southern Hemisphere truffle genus Amylascus (Pezizaceae, Ascomycota) and characterization of the sister genus Nothoamylascus gen. nov. Persoonia 51: 125–151. https://doi. org/10.3767/persoonia.2023.51.03
- Heilmann-Clausen J, Barron ES, Boddy L, *et al.* (2015). A fungal perspective on conservation biology. *Conservation Biology* **29**(1): 61–68. https://doi.org/10.1111/cobi.12388
- Hoang DT, Chernomor O, von Haeseler A, et al. (2018). UFBoot2: Improving the ultrafast bootstrap approximation. Molecular Biology and Evolution 35: 518–522. https://doi.org/10.1093/ molbev/msx281
- Hobbie EA, Rice SF, Weber NS, et al. (2016). Isotopic evidence indicates saprotrophy in post-fire *Morchella* in Oregon and Alaska. *Mycologia* **108**(4): 638–645. https://doi.org/ 10.3852/15-281
- Hobbie EA, Weber NS, Trappe JM (2001). Mycorrhizal vs saprotrophic status of fungi: The isotopic evidence. *The New Phytologist* **150**(3): 601–610. https://doi.org/10.1046/j.1469-8137.2001.00134.x
- Hopple JS, Vilgalys R (1994). Phylogenetic relationships among coprinoid taxa and allies based on data from testriction site mapping of nuclear rDNA. *Mycologia* **86**(1): 96–107. https://doi.org/10.1006/mpev.1999.0634
- Hunt M (2017). assembly-stats (1.0.1). https://github.com/sanger-pathogens/assembly-stats/
- Imai S (1933). On two new Species of *Tuberaceae*. *Proceedings of the Imperial Academy* **9**(4): 182–185. IUCN (2024).
- IUCN Red List version 2024-2: Summary Table 1a. https://www.iucnredlist.org/resources/summary-statistics Accessed on 26

- March 2025.
- Kalyaanamoorthy S, Minh BQ, Wong TKF, et al. (2017). ModelFinder: Fast model selection for accurate phylogenetic estimates. *Nature Methods* **14**:587–589. https://doi.org/10.1038/nmeth.428
- Katoh K, Asimenos G, Toh H (2009). Multiple Alignment of DNA Sequences with MAFFT. In: Posada D (ed.) Bioinformatics for DNA Sequence Analysis. *Methods in Molecular Biology*, vol 537. Humana Press. https://doi.org/10.1007/978-1-59745-251-9_3
- Kim D, Gilchrist CLM, Chun J, et al. (2023). UFCG: database of universal fungal core genes and pipeline for genome-wide phylogenetic analysis of fungi. Nucleic Acids Research 51(D1): D777–D784. https://doi.org/10.1093/nar/gkac894
- Kimbrough JW (1994). Septal ultrastructure and ascomycete systematics. In: Ascomycete Systematics: Problems and Perspectives in the Nineties (Hawksworth DL, ed). Springer, USA: 127–141.
- Komur P, Chachuła P, Kapusta J, et al. (2021). What determines species composition and diversity of hypogeous fungi in the diet of small mammals? A comparison across mammal species, habitat types and seasons in Central European mountains. Fungal Ecology 50: 101021. https://doi.org/10.1016/j. funeco.2020.101021
- Kovács GM, Trappe JM, Alsheikh AM, *et al.* (2008). *Imaia*, a new truffle genus to accommodate *Terfezia gigantea*. *Mycologia* **100**(6): 930–939. https://doi.org/10.3852/08-023
- Krpata D, Peintner U, Langer I, et al. (2008). Ectomycorrhizal communities associated with *Populus tremula* growing on a heavy metal contaminated site. *Mycological Research* 112(9): 1069–1079
- Læssøe T, Hansen K (2007) Truffle trouble: What happened to the *Tuberales? Mycological Research* **111**(9): 1075–1099. https://doi.org/10.1016/j.mycres.2007.08.004
- Lange M (1956). A new species of *Picoa. Mycologia* 48(6): 877–878.
 Lefevre C (2012). Native and cultivated truffles of North America.
 In: *Edible Ectomycorrhizal Mushrooms: Current Knowledge and Future Prospects* (Zambonelli A, Bonito GM, eds). Springer Berlin Heidelberg, Germany: 209–226.
- Leonardi P, Murat C, Puliga F, et al. (2020). Ascoma genotyping and mating type analyses of mycorrhizas and soil mycelia of *Tuber borchii* in a truffle orchard established by mycelial inoculated plants. *Environmental Microbiology* 22: 964–975. https://doi.org/10.1111/1462-2920.14777
- Li H (2018). Minimap2: pairwise alignment for nucleotide sequences.

 Bioinformatics 34:3094-3100. https://doi.org/10.1093/bioinformatics/bty191
- Li L-T (1997). Ultrastructural studies of *Leucangium carthusianum* (Hypogeous *Pezizales*). *International Journal of Plant Sciences* **158**(2): 189–197.
- Lindner DL, Banik MT (2009). Effects of cloning and root-tip size on observations of fungal ITS sequences from *Picea glauca* roots. *Mycologia* **101**(1): 157–165. https://doi.org/10.3852/08-034
- Liu W, He P, Shi X, et al. (2023). Large-scale field cultivation of Morchella and relevance of basic knowledge for its steady production. Journal of Fungi 9: 855. https://doi.org/10.3390/ jof9080855
- Liu YJ, Whelen S, Hall BD (1999). Phylogenetic relationships among ascomycetes: evidence from an RNA polymerse II subunit. *Molecular Biology and Evolution* **16**(12): 1799–1808. https://doi. org/0.1093/oxfordjournals.molbev.a026092
- Loizides M (2017). Morels: the story so far. *Field Mycology* **18**(2): 42–53. https://doi.org/10.1016/j.fldmyc.2017.04.004
- Mai U, Mirarab S (2018). TreeShrink: fast and accurate detection of



- outlier long branches in collections of phylogenetic trees. *BMC Genomics* **19** (S5): 272. https://doi.org/10.1186/s12864-018-4620-2
- Masaphy S (2010). Biotechnology of morel mushrooms: Successful fruiting body formation and development in a soilless system. Biotechnology Letters 32(10): 1523–1527. https://doi.org/10.1007/s10529-010-0328-3
- Mattirolo O (1928). Secondo elenco dei "Funghi hypogaei" raccolti nelle foreste di Vallombrosa (1900-1926). *Nuovo Giornale Botanico Italiano* **34**: 1343–1358.
- Mayor JR, Schuur EAG, Henkel TW (2009). Elucidating the nutritional dynamics of fungi using stable isotopes. *Ecology Letters* **12**(2): 171–183. https://doi.org/10.1111/j.1461-0248.2008.01265.x
- Merkus E (1976). Ultrastructure of the ascospore wall in *Pezizales* (Ascomycetes)—IV. *Morchellaceae*, *Helvellaceae*, *Rhizinaceae*, *Thelebolaceae*, and *Sarcoscyphaceae*. *Persoonia* **9**(1): 1–38.
- Miller M, Pfeiffer W, Schwartz T (2010). Creating the CIPRES Science Gateway for inference of large phylogenetic trees. *Proceedings* of the Gateway Computing Environments Workshop (GCE) **14**: 1–8.
- Miller SC (2005). Cultivation of *Morchella*. US Patent (Patent 6907691 B2).
- Minh BQ, Schmidt HA, Chernomor O, et al. (2020). IQ-TREE 2: New models and efficient methods for phylogenetic inference in the genomic era. *Molecular Biology and Evolution* **37**:1530–1534. https://doi.org/10.1093/molbev/msaa015
- Mleczko P, Kozak M, Karpowicz F (2020). New records of rare hypogeous fungi from Poland (Central Europe). *Acta Mycologica* **55**(2): 5529. https://doi.org/10.5586/am.5529
- Molia A, Larsson E, Jeppson M, et al. (2020). Elaphomyces section Elaphomyces (Eurotiales, Ascomycota) taxonomy and phylogeny of North European taxa, with the introduction of three new species. Fungal Systematics and Evolution 5(1): 283–300. https://doi.org/10.3114/fuse.2020.05.14
- Murat C, Payen T, Noel B, et al. (2018). Pezizomycetes genomes reveal the molecular basis of ectomycorrhizal truffle lifestyle. Nature Ecology, Evolution 2(12): 1956–1965. https://doi.org/10.1038/s41559-018-0710-4
- Narimatsu M, Sato S, Sakamoto Y (2023). Successful cultivation of black morel *Morchella* sp. in Japan. *FEMS Microbiology Letters* **370**: fnad101. https://doi.org/10.1093/femsle/fnad101
- Noffsinger CR, Matheny PB (2025). Historical lead contamination linked to atmospheric deposition is associated with declines in ectomycorrhizal diversity and shifts in fungal community composition. *Molecular Ecology* **34**(8): e17725. https://doi.org/10.1111/mec.17725
- O'Donnell K, Cigelnik E, Weber NS, et al. (1997). Phylogenetic relationships among ascomycetous truffles and the true and false morels inferred from 18S and LSU ribosomal DNA sequence analysis. *Mycologia* **89**(1): 48–65. https://doi.org/10.1080/00275 514.1997.12026754
- Oros-Ortega I, Andrade-Torres A, Lara-Pérez LA, et al. (2017). Ectomycorrhizal ecology biotechnology and taxonomy for the conservation and use of *Abies religiosa* in temperate areas of Mexico. *Revista Chapingo Serie Ciencias Forestales y Del Ambiente* 23(3): 411–426. https://doi.org/10.5154/r.rchscfa.2016.11.060
- Ower R (1982). Notes on the development of the morel ascocarp: *Morchella esculenta. Mycologia* **74**(1): 142–144. https://doi.org/10.2307/3792639
- Pilz D, Lefevre C, Scott L, et al. (2009). Oregon culinary truffles.

 An emergent industry for forestry agriculture culinary tourism.

- http://www.oregontruffles.org/truffles_feasibility_final.pdf Accessed on 2 February 2024.
- Paoletti G (1899). Leucangium carthusianum. In Sylloge Fungorum Omnium Hucusque Cognitorum (Saccardo PA, ed.) 8:900.
- Prjibelski A, Antipov D, Meleshko D, et al. (2020). Using SPAdes de novo assembler. *Current Protocols in Bioinformatics* **70**:e102. https://doi.org/10.1002/cpbi.102"
- Rambaut A (2018). Fig Tree v. 1.4. 4. http://tree.bio.ed.ac.uk/software/figtree/ Accessed on 1 May 2024.
- Rehner SA, Buckley E (2005). A *Beauveria* phylogeny inferred from nuclear ITS and EF1-α sequences: evidence for cryptic diversification and links to *Cordyceps* teleomorphs. *Mycologia* **97**(1): 84–98. https://doi.org/10.3852/mycologia.97.1.84
- R Core Team (2023). R: A Language and Environment for Statistical Computing. R Foundation for Statistical Computing Vienna Austria. https://www.R-project.org/ Accessed 1 May 2024.
- Reyna S, Garcia-Barreda S (2014). Black truffle cultivation: a global reality. *Forest Systems* **23**(2): 317–328. https://doi.org/10.5424/fs/2014232-04771
- Saccardo PA (1889). Sylloge fungorum omnium hucusque cognitorum (VIII) (Vol. 8). sumptibus auctoris. https://www.biodiversitylibrary.org/item/102784 Accessed 1 May 2024.
- Salvia V (2023). The Joriad 2023 North American Truffle Dog Championship: Lots of tail wagging and good food. *Eugene Magazine*. https://eugenemagazine.com/happenings/the-joriad-2023-north-american-truffle-dog-championship/ Accessed 8 May 2024.
- Schickmann S, Urban A, Kräutler K, et al. (2012). The interrelationship of mycophagous small mammals and ectomycorrhizal fungi in primeval disturbed and managed Central European mountainous forests. Oecologia 170(2): 395–409. https://doi.org/10.1007/s00442-012-2303-2
- Simão FA, Waterhouse RM, Ioannidis P, *et al.* (2015). BUSCO: Assessing genome assembly and annotation completeness with single-copy orthologs. *Bioinformatics* **31**(19): 3210–3212. https://doi.org/10.1093/bioinformatics/btv351
- Smith GR, Finlay RD, Stenlid J, et al. (2017). Growing evidence for facultative biotrophy in saprotrophic fungi: data from microcosm tests with 201 species of wood-decay basidiomycetes. *The New Phytologist* **215**(2): 747–755. https://doi.org/10.1111/nph.14551
- Sow A, Lemmond B, Rennick B, et al. (2024). Tuber cumberlandense and T. canirevelatum, two new edible Tuber species from eastern North America discovered by truffle-hunting dogs. Mycologia 116(6): 949–964. https://doi.org/10.1080/00275514.2024.24077
- Stajich JE, Palmer JM (2023). Automatic assembly for the fungi (Version 0.5.0). https://github.com/stajichlab/AAFTF Accessed 10 January 2024.
- Steindorff AS, Seong K, Carver A, et al. (2022). Diversity of genomic adaptations to the post-fire environment in *Pezizales* fungi points to crosstalk between charcoal tolerance and sexual development. *The New Phytologist* **236**(3): 1154–1167. https://doi.org/10.1111/nph.18407
- Stephens RB, Remick TJ, Ducey MJ, et al. (2017). Drivers of truffle biomass community composition and richness among forest types in the northeastern US. Fungal Ecology 29: 30–41.
- Stephens RB, Rowe RJ (2020). The underappreciated role of rodent generalists in fungal spore dispersal networks. *Ecology* 101(4): e02972. https://doi.org/10.1016/j.funeco.2017.05.004
- Stielow JB, Lévesque CA, Seifert KA, et al. (2015). One fungus which genes? Development and assessment of universal primers for potential secondary fungal DNA barcodes. *Persoonia* **35**(1):

- 242-263. https://doi.org/10.3767/003158515X689135
- Sultaire SM, Benucci GMN, Longley R, *et al.* (2023). Using high-throughput sequencing to investigate summer truffle consumption by chipmunks in relation to retention forestry. *Forest Ecology and Management* **549**: 121460. https://doi.org/10.1016/j. foreco.2023.121460
- Talavera G, Castresana J (2007). Improvement of phylogenies after removing divergent and ambiguously aligned blocks from protein sequence alignments. Systematic Biology **56**(4): 564–577. https://doi.org/10.1080/10635150701472164
- Tan H, Kohler A, Miao R, et al. (2019). Multi-omic analyses of exogenous nutrient bag decomposition by the black morel Morchella importuna reveal sustained carbon acquisition and transferring. Environmental Microbiology 21(10): 3909–3926. https://doi.org/10.1111/1462-2920.14741
- Tedersoo L, Smith ME (2013). Lineages of ectomycorrhizal fungi revisited: Foraging strategies and novel lineages revealed by sequences from belowground. *Fungal Biology Reviews* **27**(3–4): 83–99. https://doi.org/10.1016/j.fbr.2013.09.001
- Trappe JM (1971). A synopsis of the *Carbomycetaceae* and *Terfeziaceae* (*Tuberales*). *Transactions of the British Mycological Society* **57**(1): 85–92. https://doi.org/10.1016/S0007-1536(71)80083-9
- Trappe JM (1975). The genus *Fischerula (Tuberales). Mycologia* **67**(5): 934–941. https://doi.org/10.1080/00275514.1975.12019 826
- Trappe JM (1979). The orders families and genera of hypogeous Ascomycotina (truffles and their relatives). Mycotaxon 9(1): 297–340.
- Trappe JM (2009). The hunted: commercially attractive truffles native to North America. Les Champignons Forestiers Comestibles à Potentiel Commercial. In: ÉDITEUR. Biopterre ACCHF Université Laval CEF RNC 30 novembre et 1er décembre: 97–102.
- Trappe JM, Molina R, Luoma DL, et al. (2009). Diversity, ecology and conservation of truffle fungi in forests of the Pacific Northwest. United States Department of Agriculture, Forest Service Pacific Northwest Research Station General Technical Report PNW-GTR-772.
- Trappe JM, Sundberg WJ (1977). Terfezia gigantea (Tuberales) in North America. Mycologia 69(2): 433–437. https://doi.org/10.2307/3758672
- Trappe MJ, Trappe JM, Bonito G (2010). *Kalapuya brunnea gen. sp. nov.* and its relationship to the other sequestrate genera in *Morchellaceae*. *Mycologia* **102**(5): 1058–1065. https://doi.org/10.3852/09-232
- Tulasne L-R, Tulasne C (1851). Fungi hypogæi: Histoire et monographie des champignons hypogés. Parisiis apud F Klincksieck.

- Van Vooren N (2017). Leucangium carthusianum (Pezizales), la truffe de Chartreuse découverte en Auvergne. Bulletin Mycologique et Botanique Dauphiné-Savoie 226:33–38.
- Vandepol N, Liber J, Desirò A, et al. (2020). Resolving the Mortierellaceae phylogeny through synthesis of multi-gene phylogenetics and phylogenomics. Fungal Diversity 104(1): 267–289. https://doi.org/10.1007/s13225-020-00455-5
- Vasiliauskas R, Menkis A, Finlay RD, et al. (2007). Wood-decay fungi in fine living roots of conifer seedlings. *The New Phytologist* **174**(2): 441–446. https://doi.org/10.1111/j.1469-8137.2007.02014.x
- Venables WN, Ripley BD (2002). Modern Applied Statistics with S. Fourth edition. Springer New York. ISBN 0-387-95457-0 https://www.stats.ox.ac.uk/pub/MASS4/ Accessed 4 March 2024.
- Venturella G, Pecorella E, Saitta A, *et al.* (2006). Ecology and distribution of hypogeous fungi from Sicily (southern Italy). *Cryptogamie, Mycologie* **27**(3): 201–217.
- Vernes K, Blois S, Bärlocher F (2004). Seasonal and yearly changes in consumption of hypogeous fungi by northern flying squirrels and red squirrels in old-growth forest New Brunswick. *Canadian Journal of Zoology* **82**(1): 110–117. https://doi.org/10.1139/z03-224
- Větrovský T, Morais D, Kohout P, *et al.* (2020). GlobalFungi a global database of fungal occurrences from high-throughput-sequencing metabarcoding studies. *Scientific Data* **7**: 228. https://doi.org/10.1038/s41597-020-0567-7
- White TJ, Bruns T, Lee S, *et al.* (1990). Amplification and direct sequencing of fungal ribosomal RNA Genes for phylogenetics. In: *PCR Protocols: A Guide to Methods and Applications* (Innis MA, Gelfand DH, Sninsky JJ, *et al.*, eds): 315–322. Academic Press, USA.
- Wickham H (2016). ggplot2: elegant graphics for data analysis. Springer-Verlag New York. ISBN 978-3-319-24277-4 https://ggplot2.tidyverse.org Accessed on 1 May 2024.
- Yamada A (2006). "Kon-na-Kinoko-wo-tabeta—Imotake." (I ate this mushroom: *Imaia gigantea*). *Newsletter of the Mycological Society of Japan* **3**: 8–9.
- Yamamoto K, Sasaki H, Ohmae M, *et al.* (2020). *Leucangium microspermum*: Re-examination of Japanese *L. carthusianum* reveals its taxonomic novelty. *Truffology* **3**(1): 1–7.
- Zimin AV, Marçais G, Puiu D, *et al.* (2013). The MaSuRCA genome assembler. *Bioinformatics* **29**(21): 2669–2677. https://doi.org/10.1093/bioinformatics/btt476

Supplementary material

- Fig. S1. Phylogenetic analyses of LSU, tef1, and rpb2.
- Table S1. Sequence accession information and metadata.
- Table S2. Genome assembly statistics.
- Table S3. Isotopic data and QDA analysis results.